hep-ph/9602203

EVENT GENERATORS FOR DISCOVERY PHYSICS

Conveners: M.L. Mangano and G. Ridolfi

Working group: E. Accomando, S. Asai, H. Baer, A. Ballestrero, M. Besançon, E. Boos, C. Dionisi, M. Dubinin, L. Duflot, V. Edneral, K. Fujii, J. Fujimoto, S. Giagu, D. Gingrich, T. Ishikawa, P. Janot, M. Jimbo, T. Kaneko, K. Kato, S. Katsanevas, S. Kawabata, S. Komamiya, T. Kon, Y. Kurihara, A. Leike, G. Montagna, O. Nicrosini, F. Paige, G. Passarino, D. Perret-Gallix, F. Piccinini, R. Pittau, S. Protopopescu, A. Pukhov, T. Riemann, S. Shichanin, Y. Shimizu, A. Sopczak, H. Tanaka, X. Tata, T. Tsukamoto

Contents

1 Introduction

This chapter of the report presents a review of Monte Carlo (MC) event generators for signals of new particles. The areas covered include Higgs production, Supersymmetry (SUSY) and leptoquarks. Contrary to other contexts, where MC generators for specific Standard Model (SM) processes are considered, it is not possible to identify a simple common set of features which event generators for new physics should possess. Each new process presents its own theoretical and technical issues, with the emphasis being now equally shared between the precision of the calculations and the completeness of the coverage of exotic phenomena and their parametrization. While the accuracy and the statistical power of the future measurements call for high precision in the Bhabha, WW and QCD generators, a precision of the order of few percent in the determination of the cross sections for new phenomena and for their backgrounds is sufficient in most examples of practical relevance. In this respect, it is important to distinguish between two uses of event generators for new physics. The first one involves the evaluation of the potential signals, *i.e.* the calculation of production cross sections, decay branching ratios (BR's) and detector acceptances and efficiencies. The second one involves the determination of the parameters of the new physics which will be hopefully discovered from the comparison of the properties of the observed signal with what derived from the MC model. Most of the studies carried out by our working group and by the New Physics working groups covered the first issue. In the examples considered, the conclusion was that the current theoretical uncertainties in the various MC's do not affect the projected discovery potential. On the other hand the extraction of the parameters which determine the specific model of new physics could depend strongly on the accuracy of the theoretical description of the production process. For example, features such as the presence or absence of spin correlations, which do not seem to be critical for the discovery of supersymmetric particles, will affect the determination of the EW properties of the new particles, as will be shown explicitly in sect. 3.5.

The plan of this contribution is as follows: we start with Higgs production, shortly describing the main technical issues and presenting the available generators. Results and comparisons are discussed. We then present the SUSY generators, covering both multi-purpose codes which include most of the possible SUSY final states, and single-channel codes, which focus on a given signal trying to incorporate the most accurate theoretical treatment possible today. The description of a leptoquark generator will complete this work.

While this review is by no means complete, it contains most of the tools available to the public. We are aware of many other existing programs, part of which have been used in the extensive cross checks performed as part of the working group activity. Since they have not been developed for distribution, and would not be easily accessible to the public, they have not been included in this report.

2 Higgs

The search for the Higgs boson will have first priority in the LEP2 programme [1], and a large effort has been devoted to the development of reliable MC event generators. In the Standard Model, Higgs production at LEP2 is dominated by the process $e^+e^- \to Z^* \to ZH$ [1]. In the mass range of interest for LEP2 the Higgs boson is expected to decay dominantly into a pair of bottom quarks, leading to final states like $f\bar{f}b\bar{b}$, f being any fermion aside from the top. Because of the large width of the Z boson, the approximation in which the production and decay of the Z boson factorize is not good enough. On the other hand, the small width of the Higgs could justify the factorization approximation. Nevertheless, most of the event generators presented below include the matrix elements for the full 4-fermion process $e^+e^- \to f\bar{f}b\bar{b}$. The evaluation of this process involves not only the diagrams with a Higgs boson, but also all possible SM diagrams leading to the same final state. As an example, assuming $f \neq e, \nu_e$ one should evaluate a total of 25 tree level diagrams: 1 corresponding to the signal, 8 t-channel diagrams relative to ZZ, $Z\gamma$ and $\gamma\gamma$ exchange, and 16 s-channel diagrams relative to the bremstrahlung of a neutral vector boson from the fermionic final states. If f is a quark, QCD processes should be added to this last category. Likewise, different sets of diagrams appear both in the signal and in the background if $f = e$ or $f = \nu_e$. The presence of several resonating channels in the full amplitude poses some numerical problem, which can be easily overcome by choosing properly the importance sampling, as described later on. In the case of massless final state fermions, the interference between signal and background diagrams is zero, because of the helicity non-conservation induced by the coupling to the Higgs boson. If the mass of the b quarks is kept different from zero in the matrix elements, a finite interference will develop. In addition to including all diagrams, accurate event generators should also include the effects of initial state radiation (ISR), and provide the user with the effective 4-momentum of the final state after initial state photon emission. As a desirable feature, Higgs generators should also contain a description of Higgs production and decay in models beyond the SM, such as two-doublet or SUSY models [1]. Finally, one expects the code to provide unweigthed events with the 4-momenta of all final state particles, in order for the user to process the events through the detector and to apply analysis cuts.

Each code presented in this section embodies all these features to a different degree. A comparison between results obtained using different approximations will allow us to estimate the importance of any given effect, and to assess the limitation of a given approach. It must be pointed out that none of these codes contains the full 1-loop EW radiative corrections. Their evaluation and inclusion in a 4-fermion event generator has not been achieved for any 4-fermion final state. The largest component of the radiative corrections is however incorporated using the so-called Improved Born Approximation [3], in which vector boson self-energy insertions are absorbed by using running EW couplings. A partial calculation of the full EW 1-loop corrections has been performed [4] for the process $e^+e^- \to Hf\bar{f}$. The resulting production cross section never differs from the IBA by more than 2% in the range of interest at LEP2. The agreement improves for Higgs masses near the LEP2 discovery reach. The 1% level is therefore an optimal goal for the agreement between the tree level event generators which will

be described here.

2.1 CompHEP

Program name:	CompHEP – version 3.0
Authors:	E. Boos – `boos@theory.npi.msu.su`
	M. Dubinin – `dubinin@theory.npi.msu.su`
	V. Edneral – `edneral@theory.npi.msu.su`
	V. Ilyin – `ilyin@theory.npi.msu.su`
	A. Pukhov – `pukhov@theory.npi.msu.su`
	V. Savrin – `savrin@theory.npi.msu.su`
	S. Shichanin – `shichanin@m9.ihep.su`
Availability:	anonymous ftp from `theory.npi.msu.su`
	Directory: pub/comphep-3.0
	File: `30.tar.Z`
Documentation:	Files: `install.doc, manual.ps.Z`

The main purpose of CompHEP [6] is to allow the automatic evaluation of cross sections and distributions directly from an assigned lagrangian.

The general structure of the CompHEP package is described in the section "Event generators for WW physics" of this Workshop. Here we describe in more detail the feature of the program relevant for the Standard Model (SM) Higgs search at LEP2.

Any kind of three-, four- and five-particle final states can be calculated using CompHEP. In the case of Higgs boson production, the reactions of interest are $e^+e^- \to f\bar{f}b\bar{b}$, with f any lepton or quark. The main features of the calculations implemented in CompHEP can be summarized in the following way:

- all possible Feynman diagrams contributing to the process are calculated and all interferences between signal and background diagrams are taken into account (at tree level). Fermion masses can be kept nonzero in the calculation of the squared amplitudes.
- final particle phase space with massive fermions is generated explicitly.

CompHEP generates graphically complete sets of Feynman diagrams for the processes mentioned above (for instance, 25 diagrams including one signal diagram for $e^+e^- \to \mu^+\mu^-b\bar{b}$, 21 diagrams including two signal diagrams for $e^+e^- \to \nu\bar{\nu}b\bar{b}$, 50 diagrams including two signal diagrams for $e^+e^- \to e^+e^-b\bar{b}$). Any desired subset of diagrams (for instance, signal only) can be separated for further processing. Squared amplitudes and interference terms are calculated symbolically with the help of a special module for trace calculations. In the next step, optimized FORTRAN codes corresponding to these terms are generated by the package. The codes are

compiled and linked to the special interface program and Monte Carlo integrator program. The FORTRAN loading module created as a result of this process represents by itself the generator of the Higgs signal in the four fermion reaction under consideration. It is driven by the screen menu allowing the user to choose various options of signal and background simulation. A more detailed description of the menu system can be found in ref. [2].

Seven-dimensional adaptive Monte Carlo integration over the phase space and unweighted event generation is performed by the BASES/SPRING package [7]. The output has the standard BASES form (sequence of Monte Carlo iterations for total cross section and a set of histograms for various distributions). The width of the light Higgs boson is small, so the adaptive possibilities of BASES are not sufficient for integration over the phase space. Additional kinematical regularization (integration with probability density concentrated around the resonance peaks) can be introduced for the Higgs as well as vector bosons.

Initial state radiation is implemented in the structure function approach. Non-standard interaction vertices can be introduced by changing the model input (see [6] for details). Any kinematical cuts can be implemented.

At present, versions of CompHEP for different platforms exist: HP Apollo 9000, IBM RS 6000, DECstation 3000, SPARC station, Silicon Graphics and VAX.

2.2 4fan

Program name:	`4fan`
Authors:	D. Bardin – `bardindy@cernvm.cern.ch`
	A. Leike – `leike@cernvm.cern.ch`
	T. Riemann – `riemann@ifh.de`
Availability:	Anonymous ftp from `gluon.hep.physik.uni-muenchen.de:4fan`.
	Files: `4fanv12.f, 4fanv12.dat, readme`
Documentation:	D. Bardin, A. Leike and T. Riemann, Phys. Lett. **B344** (1995) 383,
	D. Bardin, A. Leike and T. Riemann, Phys. Lett. **B353** (1995) 513.

`4fan` is a semi-analytical program which calculates the process

$$e^+e^- \to f_1\bar{f}_1 f_2\bar{f}_2, \tag{2.1}$$

where the three involved fermions e, f_1 and f_2 must be in different electroweak multiplets (the so called NC32 process) [9]. SM Higgs production can be included optionally [10]. For calculations at the Born level, `4fan` can be used as a stand-alone program. For the calculation of cross sections including initial state radiation, the initial state radiation environment of the code `GENTLE` has to be used which calls `4fan` as a subroutine. For the description of `GENTLE/4fan`, we refer to [2]. Here we describe the stand-alone program `4fan`.

Six of the eight integrations of the four particle phase space were done analytically. The

two remaining integrations over $s_1 = [p(f_1) + p(\bar{f}_1)]^2$ and $s_2 = [p(f_2) + p(\bar{f}_2)]^2$ are performed numerically allowing the inclusion of cuts for these variables.

Finite mass effects are taken into account using the following approximations:

The phase space is treated exactly.

In the Higgs contributions and the conversion diagrams $e^+e^- \to (\gamma\gamma) \to f_1\bar{f}_1 f_2\bar{f}_2$, the masses are treated up to order $O[m^2(f_i)/s_i]$.

Fermion masses are treated identically in traces and Higgs couplings.

The Higgs width is calculated including the decays into b-, c- and τ- pairs.

The numbers quoted in the tables of sect. 2.8 are produced for zero fermion masses except in the Higgs couplings. The Higgs propagator is always connected with s_2 by convention.

The initialization routine `BBMMIN` assigns to the SM parameters the values from the Particle Data Book [11]. In the subroutine `DSDSHSZ`, the interferences between the three main subsets of the NC32 diagrams are calculated as well as those with the Higgs signal diagram. Their sum gives the double differential cross section. The integration of selected interferences between these subsets is not foreseen.

The numerical integration is done by a twofold application of a one-dimensional Simpson integration with a control over the relative and the absolute error. The singularities due to resonating vector propagators are eliminated by appropriate changes of integration variables. To avoid numerical instabilities, the kinematical functions resulting from the six-fold analytical integration are replaced by Taylor expansions near the borders of the phase space. The shortest calculational time is achieved by a choice of the required absolute and relative errors in such a way that they give approximately equal contributions to the error of the output.

The calculational time of a Born cross section is several seconds on a HP workstation depending on the required accuracy and on the cuts on s_1 and s_2; improving the accuracy by a factor of ten approximately doubles the calculational time.

Input and output are transferred through the arguments of the subroutine only.

Usage of the program:

```
CALL FOURFAN(EPS,ABS,IF1,IF2,S,S1MIN,S1MAX,S2MIN,S2MAX,AMH,IOUT,OUT)
```

Input:

`EPS,ABS:`		The required relative and absolute error. If at least one of the two criteria is fulfilled, the calculation is finished.
`IF1,IF2:`		Integers specifying the two final fermion pairs according to the Monte Carlo particle numbering scheme, see Particle Data Group [11], Chapter 32).
`S:`		The c.m. energy squared of the e^+e^- pair.
`S1MIN,S1MAX:`		The integration bounds of s_1.
`S2MIN,S2MAX:`		The integration bounds of s_2.
`AMH:`		The Higgs mass.
`IOUT:`		Integer, selecting the output, Currently `IOUT`=1, 2, 11 and 12 are implemented:
	`IOUT=1:`	Total cross section σ_t without Higgs.
	`IOUT=2:`	Differential cross section $\mathrm{d}\sigma/\mathrm{d}s_2$ without Higgs.
	`IOUT=11, 12:`	The same as `IOUT=1, 2` but *with* Higgs.

The units of the input (if required) are GeV^2 or GeV.

Output: `OUT` Depends on the value of `IOUT`. The output is given in fb or in fb/GeV.

On HP workstations `4fan` must be compiled with the -K option.

2.3 HIGGSPV

Program name:	HIGGSPV
Authors:	G. Montagna – `montagna@pv.infn.it`
	O. Nicrosini – `nicrosini@vxcern.cern.ch`
	F. Piccinini – `piccinini@pv.infn.it`
Availability:	Code available upon request
Documentation:	

General Description. The present version of the four-fermion Monte Carlo code HIGGSPV is an upgrade of the version used in [12], where a general description of the formalism adopted and the physical ideas behind it can be found (see also references therein). All the physical and technical upgrades will be described in detail in [13].

The program is based on the exact tree-level calculation of several four-fermion final states relevant for Higgs search at future e^+e^- colliders. Any cut on the final state configuration can be implemented. Initial- and final-state QED corrections are taken into account at the leading logarithmic level by proper structure functions, including p_T/p_L effects [23]. An hadronization interface is under development. All the relevant presently known non-QED corrections are also taken into account.

Features of the program. The code consists of three Monte Carlo branches, in wich the

importance-sampling technique is employed to take care of the peaking behaviour of the integrand:

- Unweighted event generation. The code provides a sample of unweighted events, defined as the components of the four final-state fermions momenta, plus the components of the initial- and final-state photons, plus $\sqrt{s}$, stored into proper n-tuples. The code returns also the value of the unweigthed-event cross section, together with a Monte Carlo estimate of the error. The program must be linked to CERNLIB for graphical interfaces.
- Weighted event integration. It is intended for computation only. In particular, the code returns the value of the cross section for weighted events together with a Monte Carlo estimate of the errors. The program must be linked to CERNLIB for the evaluation of few special functions.
- Adaptive integration. It is intended for computation only, but offering high precision performances. On top of importance sampling, an adaptive Monte Carlo integration algorithm is used. The program must be linked to NAG library for the Monte Carlo adaptive routines. Full consistency between non-adaptive and adaptive integrations has been explicitely proven. Neither final-state radiation nor p_T splitting are taken into account in this branch.

The non-adaptive branches rely upon the random number generator RANLUX.

The most important features are:

- The processes available are the neutral current reactions $e^+e^- \to l\bar{l}q\bar{q}$, namely NC48 (NC50 = NC48 + Higgs signals) NC24 (NC25 = NC24 + Higgs signal), NC19 (NC21 = NC19 + Higgs signals).
- Any kind of cuts can be imposed.
- There is the possibility of getting information on the contribution of subsets of the diagrams by setting proper flags.

At present, final state decays are not implemented and finite fermion mass effects are partially taken into account at the phase space boundary. However it is worth noting that the $\mathcal{O}(\alpha_s^2)$ running quark masses ($m_{c,b}(m_H^2)$) are employed in the $Hq\bar{q}$ coupling. An interface to hadronization packages is presently under development.

How the code works. After the initialization of the SM parameters and of the electromagnetic quantities, the independent variables are generated, according to proper multi-channel importance samplings, within the allowed phase space. By means of the solution of the exact kinematics, the four-momenta of the outgoing fermions, together with the four-momenta of all the generated photons, are reconstructed in the laboratory frame. If the event satisfies the cuts

imposed by the user in SUBROUTINE CUTUSER the matrix element is called, otherwise it is set to zero.

In the generation branch, an additional random number is generated in order to implement the hit-or-miss algorithm and if the event is accepted it is recorded into an n-tuple. In the non-adaptive integration branch, the cross section for weighted events is computed. In the adaptive integration branch (ref.: NAG routine D01GBF), on top of importance sampling the integration routine automatically subdivides the integration region into subregions and iterates the procedure where the integrand is found more variant. The program stops when a required relative precision is achieved.

Input parameters and flags. A sample of input flags that can be used is the following:

`OGEN = I` choice between integration [I] and generation [G] branch

`RS =` c.m. energy (GeV)

`OFAST = N` choice between adaptive [Y] or non adaptive [N] branch

`NHITWMAX =` number of weighted events

`IQED = 1` choice fo Born [0] or QED corrected [1] predictions

`OSIGN = Y` includes [Y] or does not include [N] the Higgs-boson signal

`OBACK = Y` includes [Y] or does not include [N] the SM background

`NSCH = 2` Renormalization Scheme choice (three possible choices)

`ALPHM1 = 128.07D0` $1/\alpha$ value (LEP2 standard input)

`ANH =` the Higgs-boson mass (GeV)

`OBS = 1` option for the required $l\bar{l}q\bar{q}$ channel

The Higgs-boson width is calculated including the decays into c, τ and b pairs. A detailed account of the other relevant possibilities offered by the code (namely, command files for generation and adaptive integration branches) will be given elsewhere [13].

Description of the output. For all three branches the output contains the values of the relevant Standard Model parameters. In the generation branch, an n-tuple containing the generated events is written, in addition to the output file containing the values of the cross sections for unweighted events. In the integration branches, the values of the cross sections with their numerical errors are printed.

2.4 HZHA

Program name:	HZHA
Author:	P. Janot – `janot@cernvm.cern.ch`
Availability:	`JANOT 193` minidisk on `CERNVM`.
	Files `HZHA FORTRAN`, `HZHA CARDS` and `HZHA EXEC`.
Documentation:	

General description. This generator is designed to provide a complete coverage of possible production and decay channels of SM (h) and MSSM (h, H, A) Higgs bosons at e^+e^- colliders. The complete set of background four-fermion processes is however not included. HZHA allows eight different Higgs production processes to be simulated (only the processes 1, 5 and 7 are relevant for the SM):

1. $e^+e^- \to hZ \to hf\bar{f}$,
2. $e^+e^- \to HZ \to Hf\bar{f}$,
3. $e^+e^- \to hA$,
4. $e^+e^- \to HA$,
5. $e^+e^- \to \nu\bar{\nu}h$ *via* WW fusion,
6. $e^+e^- \to \nu\bar{\nu}H$ *via* WW fusion,
7. $e^+e^- \to e^+e^-h$ *via* ZZ fusion,
8. $e^+e^- \to e^+e^-H$ *via* ZZ fusion,

No interference between these channels is as yet included. The following decay modes of each Higgs boson are considered:

1. $\gamma\gamma$	2. gg	3. $\tau^+\tau^-$	4. $c\bar{c}$
5. $b\bar{b}$	6. $t\bar{t}$	7. $W^{+*}W^{-*}$	8. Z^*Z^*
9. $h,H \to AA$, with $A \to Zh$	10. $H \to hh$	11. γZ^*	12. e^+e^-
13. $\mu^+\mu^-$	14. $s\bar{s}$	15. $\tilde{\chi}\tilde{\chi}$	16. $\tilde{\chi}^+\tilde{\chi}^-$.

The squark, slepton, chargino, neutralino masses and mixings are computed in the MSSM framework. The squarks and sleptons are assumed to be sufficiently heavy that no Higgs boson can decay to them. However, decays to $\tilde{\chi}^0$'s and $\tilde{\chi}^\pm$'s are enabled when kinematically allowed. Therefore, the branching ratios of charginos and neutralinos are also computed and their decays simulated in the following channels :

1. $\tilde{\chi}_2^0 \to \tilde{\chi}_1^0 Z^* \to \tilde{\chi}_1^0 f\bar{f}$,

2. $\tilde{\chi}_2^0 \to \tilde{\chi}^+ \mathrm{W}^{-*} \to \tilde{\chi}_1^0 \mathrm{f}\bar{\mathrm{f}}'$,

3. $\tilde{\chi}_2^0 \to \tilde{\chi}_1^0 \gamma$,

4. $\tilde{\chi}^+ \to \tilde{\chi}_1^0 \mathrm{W}^* \to \tilde{\chi}_1^0 \mathrm{f}\bar{\mathrm{f}}'$,

where $\tilde{\chi}_1^0$ and $\tilde{\chi}_2^0$ are two lightest neutralinos, and $\tilde{\chi}^+$ is the lightest chargino (with $m_{\tilde{\chi}_2^0}, m_{\tilde{\chi}^+} > m_{\tilde{\chi}_1^0}$). Cascade decays are also simulated. The lightest neutralino $\tilde{\chi}_1^0$ is assumed to be the LSP (if not so, a warning message appears and the program may stop) and R-parity is assumed to be conserved.

In the SM the $\mathrm{h} \to \tilde{\chi}\tilde{\chi}$ is allowed to simulate invisible Higgs decays. In the MSSM, the $\gamma\gamma$ and $\gamma\mathrm{Z}$ (resp. gg) decay widths are computed with all the charged (resp. coloured) particles in the loops (squarks, leptons, charginos, charged Higgses).

Finally, the MSSM Higgs boson pole masses are computed using by default the improved renormalization group equations at two loops [14] (they may also be computed using the EPA for comparison purposes). An independent computation of Higgs masses [15] will be implemented soon.

Features of the program. `HZHA` is an event generator based on a Monte-Carlo technique, producing any desired combination of the final states listed above. In addition, any Z decay channel combination can be defined by the users for the processes 1 and 2 ($\mathrm{e}^+\mathrm{e}^- \to \mathrm{hZ}$ and HZ).

The initial state radiation (ISR) is implemented by means of the REMT package by R. Kleiss, modified to account for the α^2 part of the spectrum, and the possibility of the radiation of two initial photons. The final state radiation (FSR) is implemented for the leptonic Z decays in the processes 1 and 2.

All final state fermions are massive. The couplings of the Higgs bosons to the quarks are computed using the two-loop running quark masses evolved to the Higgs boson mass scale. The pole masses chosen for the c- and the b-quark are 1.64 and 4.87 GeV/c^2. More generally, the cross-sections for all requested processes and the decay widths/branching ratios for all three Higgs bosons are computed with all known QED, weak and QCD corrections. In particular, Higgs width effects are taken into account both in the cross-section computation and in the event generation. Finally, the program is fully interfaced with `JETSET 7.4` [16] for the hadronization of the final state quarks.

How it works. When the program is called, the initialization part determines the relevant masses, mixing and couplings as mentioned above, computes the decay widths and branching ratios for the Higgs bosons, the neutralinos and the charginos, and gives the total production cross-sections without and with ISR.

Unweighted events are generated according to the user requests (number of events to be generated, choice of the production processes and the decay channels,...). The events are

stored in the LUJETS common blocks for subsequent use, e.g. in an interface with full detector simulation.

The job is closed by some statistics printout (numbers of events generated in each of the processes and of the decay channels).

Input parameters, flags, etc. The inputs are chosen by the user through data cards read by the CERNLIB routine FFREAD. See item 8 to see where the card file can be obtained from. This card file is well documented and self explanatory. The following inputs can be freely set:

1. From the card TRIG, the first and last events to be generated;
2. From the card DEBU, the first and last events to be printed out;
3. From the card TIME, the time to keep at the end of the job;
4. From the card GENE, the general parameters (centre-of-mass energy, ISR flag, SM or MSSM flag...);
5. From the card GSMO, the SM parameters (Z mass and width, Fermi constant, top mass, Higgs boson mass $m_{\rm H}$, $\Lambda^{(5)}_{QCD}$);
6. From the card GSUS, the MSSM parameters ($m_{\rm A}$, $\tan\beta$, the universal gaugino mass M, the squark mixing parameters μ, $A_{\rm t}$, $A_{\rm b}$, and the masses m_Q, m_U, m_D, m_L, m_E);
7. From the card PRYN, the process(es) to be generated;
8. From the card GZDC, the Z decay channels to be enabled;
9. From the card GCH1, the H decay channels to be enabled;
10. From the card GCH2, the h decay channels to be enabled (also used for the SM Higgs boson);
11. From the card GCH3, the A decay channels to be enabled;

Other data cards can be added (in which case the program should be modified to be able to understand them) to set branching ratios, masses, widths of particles for the JETSET running.

A description of the output to be expected. The output contains the values of the Higgs boson production cross-sections and decay branching ratios, followed by the listing of the numbers of events given by the data card DEBU, and terminated by the end-of-run statistics.

Where can the program be obtained? The program (and its subsequent updates) can be obtained upon request by e-mail to janot@cernvm.cern.ch. It can also be found, for the time being, on the JANOT 193 minidisk on CERNVM. Relevant files are named HZHA FORTRAN and HZHA CARDS. An example of EXEC file (HZHA EXEC) can also be found at the same place.

2.5 PYTHIA

Program name:	PYTHIA – version 5.720, 29 November 1995
Author:	T. Sjöstrand – `torbjorn@thep.lu.se`
Availability:	http://thep.lu.se/tf2/staff/torbjorn/Welcome.html
Documentation:	address above and Comp. Phys. Commun. 82 (1994) 74

PYTHIA [16] is a general-purpose event generator, with emphasis on a complete description of QCD cascades and hadronization. Therefore it is extensively discussed in the QCD generators report of this report. Among its selection of subprocesses, described there, there are several related to Higgs production (signal and backgrounds). Extensive details can be found in the documentation referred to above.

2.6 WPHACT

Program name:	WPHACT
Authors:	E. Accomando – `accomando@to.infn.it`
	A. Ballestrero – `ballestrero@to.infn.it`
Availability:	Anonymous `ftp` from:
	`ftp.to.infn.it:pub/ballestrero`
Documentation:	To be found in the above directory.

General description. WPHACT is a program created to study four fermion, WW and Higgs physics at present and future e^+e^- colliders. In its present form, it can compute all SM processes with four fermions in the final state.

We will give here a description of the program and his characteristics with particular emphasis to those regarding Higgs physics. We refer to the analogous description in the WW Physics section of this report for what concerns charged current processes and some general features of the program.

For all processes with $b\,\bar{b}$ in the final state together with $\mu\bar{\mu}$, $\nu_\mu\bar{\nu}_\mu$, $\nu_e\bar{\nu}_e$ and $b\,\bar{b}$, finite b masses are properly taken into account both in the phase space and in matrix elements. Higgs contributions are of course included.

Full tree level matrix elements for these processes (as well as for all other four fermion final states) are computed by means of subroutines which make use of the helicity formalism of ref. [17], which is particularly suited for treating massive fermion processes. The code for them has been written semi automatically through the set of routines PHACT [18] (**P**rogram for **H**elicity **A**mplitudes **C**alculations with **T**au matrices) which implements the method in a fast and efficient way. In the above formalism, eigenstates of the fermion propagators are used to simplify matrix expressions. These eigenstates are chosen to be generalizations of the spinors used in ref. [19]. With the introduction of so called tau matrices [17], the numerators of fermion

propagators have a very simple expression also in the massive case and one does not have to care about the various mass terms. The computation of fermion lines reduces to evaluating the matrices corresponding to insertions of vector or scalar lines and combining them together. The program PHACT writes automatically the optimized FORTRAN code necessary for every insertion and every combination, given the names of the vectors, couplings, etc. It turns out that the massive case is not more complicated than the massless one. Only more helicity indices are of course needed. As a consequence, the codes for massive amplitudes written in this way are not much slower, as it is normally the case, than those with massless fermions.

The user has the choice among three different ways of sampling the phase space, in order to take into account the peak structure of the Higgs signal and of the other resonating diagrams of the background. The adaptive routine VEGAS [20] is used for integrating over the phase space.

Features of the program. WPHACT is a Monte Carlo program. The integration is performed by VEGAS [20]. For all phase spaces used, all momenta are explicitly computed in terms of the integration variables. This implies that any cut can be implemented, and it can be easily used also as an event generator. The events obtained in this way are of course weighted. Distributions for any variable can also be easily implemented, even if no automatic implementation of distributions has yet been introduced.

All final states computed by WPHACT correspond to four fermions. Thus no stable Z or Higgs are allowed in the final state. They are always considered as virtual particles. The Higgs decay particles are always treated as massive, both in the matrix elements of signal and background and in the phase space. All tree level QCD background processes ($\mathcal{O}(\alpha\ \alpha_s)$) leading to four-quark final states are completely taken into account. Initial state QED radiation is included through structure functions $\mathcal{O}(\alpha^2)$. Anomalous gauge boson couplings are also present, if required. FSR is not implemented and no interface to hadronization is available.

It is easy to obtain contributions from different set of diagrams, as every diagram is evaluated individually for all helicity configuration and then summed to the others before squaring and summing over helicity configurations. In particular contributions to Higgs signal, background and their interference can be evaluated separately.

We give some indicative values about the running time on an ALPHA AXP 2100/4 OVMS, in the massive case:

CPU time per call for $e^+e^- \to b\bar{b}b\bar{b}$ Higgs signal with ISR: 3.0×10^{-4} sec.

CPU time per call for $e^+e^- \to b\bar{b}b\bar{b}$ Higgs background with ISR: 1.3×10^{-3} sec.

CPU time per call for $e^+e^- \to b\bar{b}\mu^+\mu^-$ Higgs signal with ISR: 9.0×10^{-5} sec.

CPU time per call for $e^+e^- \to b\bar{b}\mu^+\mu^-$ Higgs background with ISR: 6.3×10^{-4} sec.

For the same processes without ISR, CPU time per call is about 20% less. On a VAXstation 4000/90 CPU time for these programs has to be multiplied approximately by a factor 5.

At LEP2 energies, 2.5 M calls (about 13 minutes for the first process and 4 minutes for the second one) are used on ALPHA AXP to obtain Higgs signal with ISR cross section with a typical estimated error of about 1×10^{-4}. The same processes can be evaluated in about 1.5 minutes and 15 sec. respectively with 0.2 M calls at permill level. At this level 2.5 M calls (30 minutes) are necessary for $e^+e^- \to b\bar{b}\mu^+\mu^-$ Higgs background with ISR while 16 M calls (6 hours) are needed for $e^+e^- \to b\bar{b}b\bar{b}$ Higgs background with ISR.

How the code works. The variables which parametrize the phase space are: the masses of the two virtual Z's (or those of the virtual Higgs and Z), the angle of the two particles with respect to the beam, the decay angles in their rest frames, and x_1, x_2, the fractions of momenta carried by the electrons. Appropriate changes of variables to optimize the sampling of the peaks in x_1, x_2, M_H and M_Z lead to the actual integration variables. For every point chosen by the integration routine, the full set of four momenta are reconstructed and passed to the subroutine which evaluates the differential cross section with the helicity amplitude formalism. For every point in the integration variables, i.e. for every set of four momenta chosen, VEGAS gives a weight which can be used together with the value of the cross section for producing distributions.

Three different ways of sampling the massive phase space are available, which are appropriate for different peaking structures. We can classify them as double resonant, single resonant and non resonant. We have verified that normally the double resonant phase space is accurate enough. The other two can be used to study contributions of a particular subset of diagrams. It is better to run the Higgs signal and background separately, adding the results, as the change of variables necessary to take care of the resonances of the two contributions depends on their masses. The interference is normally added to the background, but it can be separated and evaluated by itself.

The $e^+e^- \to b\bar{b}b\bar{b}$ is in principle a little more complicated to integrate than processes with only one pair of b's in the final state. This is due to the presence of identical particles in the final state which implies that each b can be resonating in some diagrams with the first $\bar{b}$ and in others with the second one. This further complicates the subdivision in double resonant contributions, but we have reduced it to the simpler cases just exploiting the symmetries of the problem. This simplification is exact only in the symmetric case. One cannot thus evaluate at present the four b processes with cuts which are not symmetric under the exchange of the two b's or of the two $\bar{b}$'s among themselves. A cut which does not fulfill the above requirement is in any case unphysical.

After every iteration the integration routine readjusts the grid in the space of integration variables, in order to concentrate evaluations of the integrands in those regions where the integrand is larger in magnitude. It is advised to use a first iteration with few points to "thermalize".

Input parameters, flags, etc. The standard input parameters are M_H, M_W, M_Z, M_b, α, α_s. In the tuned comparisons presented in sect 2.8 $\sin^2\theta_W$ has been given as an input, while it is usually derived from the relation $\sin^2\theta_W = 1 - M_W^2/M_Z^2$.

The main flag of the program is `ich`, which chooses among different final states. Other flags allow to compute with or without ISR (`isr`), to choose among signal, background and interference (`isig`), and to choose whether or not to use some thermalizing iterations (`iterm`). The number of iterations (`itmx`) and of points per iteration (`ncalls`) for the thermalizing phase as well as for the normal one and the accuracy required (`acc`) are read from the input.

Output. The output is just the standard VEGAS output, from which one can read the final result and estimated statistical error, as well as the result and error for every iteration. Results with big oscillations among different iterations and corresponding big reported χ^2 have to be discarded and simply mean that the number of evaluations per iteration was not sufficient for the integrand.

Concluding remarks. As already stated, WPHACT makes use of matrix elements which are suitable for massive fermion calculations. One may question how big the mass effects are for Higgs physics. Using WPHACT one can verify that they are normally at the percent level. They however depend on the Higgs mass, and expecially on the cuts introduced. These may change the expected dependence, and any set of realistic cuts has to be studied independently with programs which take masses into account.

WPHACT does not make use of any library, has proven to be reliable over a vast range of statistical errors and can compute in short time exact massive processes of interest for Higgs physics at e^+e^- colliders.

2.7 WTO

Program name:	WTO
Author:	G. Passarino – `giampiero@to.infn.it`
Availability:	
Documentation:	

WTO is a *quasi-analytical, deterministic* code for computing observables related to the process $e^+e^- \to \bar{f}_1 f_2 \bar{f}_3 f_4$. The full matrix elements are used and in the present version the following final states are accessible (see [21] for a general classification):

1. CC3, CC11, CC20
2. NC19, NC24, NC32
3. NC21 (= NC19 + Higgs), NC25 (= NC24 + Higgs)
4. MIX43

Further extensions will be gradually implemented. To fully specify WTO's setup an option must be chosen for the renormalization scheme (RS). One has:

1. the option commonly used for tuned comparisons, i.e.

$$s_W^2 = \frac{\pi\alpha(2M_W)}{\sqrt{2}G_\mu M_W^2}, \qquad g^2 = \frac{4\pi\alpha(2M_W)}{s_W^2} \tag{2.2}$$

2. or the default,

$$s_W^2 = 1 - \frac{M_W^2}{M_Z^2}, \qquad g^2 = 4\sqrt{2}G_\mu M_W^2 \tag{2.3}$$

where $\alpha^{-1}(2M_W) = 128.07$ and G_μ is the Fermi coupling constant. Final state QCD corrections are not taken into account in the present version, but for the Higgs width. A more complete description of WTO is given in ref. [2].

Among all four-fermion processes included in WTO [2], those of relevance to Higgs physics are:

$$e^+e^- \to \bar{b}b\bar{X}X, \qquad (X = l, q \neq b) \tag{2.4}$$

The matrix elements are obtained with the helicity method described in [26]. The whole answer is written in terms of invariants, i.e.

$$e^+(p_+)e^-(p_-) \to f(q_1)\bar{f}(q_2)f'(q_3)\bar{f}'(q_4), \tag{2.5}$$

$$x_{ij}s = -\left(q_{i-2} + q_{j-2}\right)^2, \quad x_{1i}s = -\left(p_+ + q_{i-2}\right)^2, \tag{2.6}$$

$$x_{2i}s = -\left(p_- + q_{i-2}\right)^2, \quad s_1 s^2 = \epsilon\left(p_+, p_-, q_1, q_2\right), \ldots \tag{2.7}$$

and the integration variables are chosen to be

$$m_-^2 = x_{24}, \quad m_+^2 = x_{56}, \quad M_0^2 = x_{45}, \quad m_0^2 = x_{36}, \tag{2.8}$$

$$m^2 = x_{35}, \quad t_1 = x_{13}, \quad t_W = x_{13} + x_{14} \tag{2.9}$$

The convention for the final states in WTO is: $e^+e^- \to 1 + 2 + 3 + 4$. For CC processes $1 = d, 2 = \bar{u}, 3 = u', 4 = \bar{d}'$, with $u = \nu, u, c$ and $d = l, d, s, b$. For NC processes the adopted convention is $1 = f, 2 = \bar{f}, 3 = f'$ and $4 = \bar{f}'$. Initial state QED radiation is included through the Structure Function approach up to $O(\alpha^2)$. The code will return results according to three (pre-selected) options, i.e $\beta^2\eta$ (default) [22], β^3 [23] and $\beta\eta^2$ [24] where

$$\beta = 2\,\frac{\alpha}{\pi}\left(\log\frac{s}{m_e^2} - 1\right), \qquad \eta = 2\,\frac{\alpha}{\pi}\log\frac{s}{m_e^2} \tag{2.10}$$

When initial state QED radiation is included there are two additional integrations over the fractions of the beam energies lost through radiation, $x_\pm$. This description of the phase space gives full cuts-availability through an analytical control of the boundaries of the phase space. Upon specification of the input flags it is therefore possible to cut on all final state invariant masses, all (LAB) final state energies $E_i, i = 1,4$, all (LAB) scattering angles, $\theta_i, i = 1,4$, all (LAB) final state angles, $\psi_{ij}, i, j = 1,4$. Both the matrix elements and the phase space are given for massless fermions. There is no interface with hadronization. The integration is performed

with the help of the NAG routine D01GCF. This routine uses the Korobov-Conroy number theoretic approach with a MC error estimate arising from converting the number theoretic formula for the n-cube $[0,1]^n$ into a stochastic integration rule. This allows a 'standard error' to be estimated. Prior to a call to D01GCF the peak structure of the integrand is treated with the appropriate mappings. The typical process considered belong to the NC21 or NC25 classes. In WTO both the phase space and the matrix elements are written for massless fermions, thus there is no interference between the Higgs signal and the background, making particularly easy to include the Higgs boson. The pole quark masses are specified in a DATA BLOCK as $m_q(m_q^2)$ and the code will convert them internally into running masses, i.e. $m_q(m_H^2)$. Whenever needed the input parameter $\alpha_s(M_W)$ is also converted into $\alpha_s(m_H^2)$. The obtained $m_q(m_q^2)$ are then used to generate the couplings $H \to \bar{q}q$. The Higgs width is computed as $\Gamma_H = \Gamma(H \to \tau^+\tau^-, \bar{c}c, \bar{b}b, gg)$ and upon proper initialization of the corresponding flag final state QCD corrections are applied.

Numerical input parameters such as $\alpha(0), G_\mu, M_z, M_W, \ldots$ are stored in a BLOCK DATA. There are various flags to be initialized to run WTO. Here follows a short description of the most important ones:

`NPTS` - INTEGER, NPTS=1,10 chooses the actual number of points for applying the Korobov-Conroy number theoretic formulas. The built-in choices correspond to to a number of actual points ranging from 2129 up to 5,931,551.

`NRAND` - INTEGER, NRAND specifies the number of random samples to be generated in the error estimation (usually $5-6$).

`OXCM` - CHARACTER*1, the main decision branch for the process: [C(N)] for CC,(NC) [21].

`OTYPEM` - CHARACTER*4,Specifies the process, i.e. CC3, CC11, CC20 for CC processes and NC19, NC24, NC21, NC25, NC32 for NC processes.

`IOS` - INTEGER, two options $[1,2]$ (1 =default for tuned comparisons) for the RS.

`IOSF` - INTEGER, three options $[1-3]$ for the $\eta - \beta$ choice in the structure functions.

CHDM... - REAL, Electric charges, third component of isospin for the final states.

WTO is a robust one call - one result code, thus in the output one gets a list of all relevant input parameters plus the result of the requested observable with an estimate of the numerical error. A very rough estimate of the theoretical error (very subjective to say the least) can be obtained by repeating runs with different IOS, IOSF options. After the following initialization:

```
7 6                    !  NPTS NRAND
175.d0                 !  E_CM OF PROCESS
n                      !  NC PROCESS
```

```
nc25                        !  CLASS = NC25
l                           !  MU
65.d0                       !  M_H(GEV)
0.12d0                      !  ALPHA_S(M_W)
y                           !  FS QCD
y                           !  H --> GG INCLUDED
1 1                         !  IOS IOSF
hc                          !  BUILT-IN CHOICE OF CUTS
hl                          !                    "
-1.d0 -0.33333333333d0      !  CHARGES: F=MU, FP=B
-0.5d0 -0.5d0               !  ISOSPINS
1.d0 3.d0                   !  COLOR FACTORS
```

corresponding to the process for $e^+e^- \to \mu^+\mu^-\bar{b}b$ with $M_z - 25\,\mathrm{GeV} < M_{\nu\nu} < M_z + 25$ GeV, $M_{\bar{b}b} > 50$ GeV, the typical output will look as follows:

```
This run is with:

NPTS         =  7
NRAND        =  6

E_cm (GeV) =          0.17500E+03
beta       =          0.11376E+00 sin^2     =          0.23103E+00
M_W  (GeV) =          0.80230E+02 M_Z (GeV) =          0.91189E+02
G_W  (GeV) =          0.20337E+01 G_Z (GeV) =          0.24974E+01
M_H  (GeV) =          0.65000E+02 G_H (MeV) =          0.15865E+01

m_b(M_H) (GeV) =          0.29168E+01
m_c(M_H) (GeV) =          0.64862E+00
alpha_s(M_H)   =          0.12402E+00

nc25-diagrams : charges    -1.0000   -0.3333
                isospin    -0.5000   -0.5000

On exit IFAIL = 0 - Cross-Section

CPU time  28 min  37 sec, sec per call  =  0.286E-02
# of calls      =     599946

(Signal) sigma  =  0.2766804E-01   +-          0.1188170E-04
```

```
Rel. error of      0.043 %
```

2.8 Comparisons among the programs

In this section we present some "tuned" comparisons between semianalytical/deterministic and Monte Carlo codes for Higgs searches. In the case of SM Higgs production, we will consider the following processes:

$$\begin{aligned} e^+e^- &\to b\bar{b}\mu^+\mu^- \\ e^+e^- &\to b\bar{b}\nu_\mu\bar{\nu}_\mu \\ e^+e^- &\to b\bar{b}\nu_e\bar{\nu}_e. \end{aligned} \tag{2.11}$$

The selection criteria adopted involve only invariant-mass cuts, in order to allow also some semianalytical approaches to appear in the comparisons. These cuts are: $M_Z - 25$ GeV $\leq m_{l\bar{l}} \leq M_Z + 25$ GeV; $m_{b\bar{b}} \geq 50$ GeV. Cross section values for different beam energies and different Higgs masses are given in Tables 1 – 12. As a reference, the last column of each Table contains the cross sections in absence of Higgs signal (pure 4-fermion background). The results of the pure non-Higgs channels obtained by the EXCALIBUR [2] and FERMISV[1] [27] code are also shown. The input parameters used in these Tables are the *STANDARD LEP2 INPUT* [2]. The only exception is the choice of fermion masses. Since the $H \to f\bar{f}$ coupling constant is proportional to m_f, the choice adopted here [1] is to use running fermion masses $m_f = m_f(Q^2 = m_H^2)$ in the Higgs-boson coupling [1]. The codes which can evaluate massive amplitudes (CompHEP, GENTLE/4fan and WPHACT), adopt however different prescriptions for the choice of the b mass appearing in the phase space and in the matrix elements. For example, WPHACT can fix this to be the pole mass, while GENTLE/4fan adopts the same value used for the coupling to the Higgs. The suffix added to the results of the CompHEP and WPHACT programs refers to the value of the b quark mass used in the evaluation of the *production* matrix elements. The effect of the complete inclusion of b-masses in the matrix elements is clearly visible from the Tables, although it never exceeds the % level.

Few comments on the results are in order. With the exception of HZHA, which does not include the full set of SM background diagrams, the agreement between the Higgs codes presented in the Tables is systematically at the level of 1% or better. The exceptions are the processes with $\nu_e\bar{\nu}_e$ in the final state, where CompHEP differs by approximately 2% from the other codes (see Table 5 and 6). Notice that this is the channel where the difference between having and not having the full set of SM diagrams is potentially the largest, as indicated by the results of HZHA, which can differ from the other codes by up to 20%. While discrepancies at the % level are of the order of the net uncertainty coming from higher order corrections, it is clear that they should be studied further in order to make any future full NLO result meaningful. At the same time, it is important to point out that the impact of the discrepancies

[1]The numbers for FERMISV were kindly generated by P. Janot.

we found on the discovery potential of LEP2 is minimal. Whether these differences could affect the extraction of Higgs properties after its discovery at LEP2 is an interesting question, which however will require further work to be answered.

m_H (GeV)	65	90	115	∞
CompHEP_0	32.487(63)	1.593(03)	1.059(02)	1.059(02)
$\text{CompHEP}_{4.7}$	32.474(63)	1.578(03)	1.046(02)	1.046(02)
EXCALIBUR	—	—	—	1.0594(03)
FERMISV	—	—	—	0.931(22)
GENTLE/4fan	32.7148(33)	1.59930(16)	1.05949(11)	1.05944(11)
HIGGSPV	32.714(27)	1.607(08)	1.060(02)	1.049(07)
HZHA	32.435(33)	1.570(33)	1.056(33)	1.056(33)
$\text{WPHACT}_{4.7}$	32.5604(66)	1.58552(62)	1.04684(56)	1.04679(55)
WPHACT_0	32.7141(68)	1.59946(64)	1.05953(56)	1.05948(56)
WTO	32.7268(51)	1.5980(13)	1.0582(12)	1.0581(12)

Table 1: $\sigma(e^+e^- \to \mu^+\mu^- b\bar{b})$ (fb) at $E_{cm} = 175$ GeV. No ISR.

Only one of the codes presented here (HZHA) allows the generation of SUSY Higgs bosons. We present a set of cross sections for the $e^+e^- \to b\bar{b}b\bar{b}$ final state for the four cases relative to the following choice of parameters [1]:

(1) $m_A = 75$ GeV , $\tan\beta = 30$;
(2) $m_A = 400$ GeV , $\tan\beta = 30$;
(3) $m_A = 75$ GeV , $\tan\beta = 1.75$;
(4) $m_A = 400$ GeV , $\tan\beta = 1.75$.

The SM input parameters are the same as for the previous comparisons, and all the $b\bar{b}$ pairs are required to have $m_{b\bar{b}} \geq 20$ GeV. The results are shown in Tables 13 – 16. The only comparison possible between the results of HZHA and those of other codes is for the SM backgrounds. For these we present, when available, the separate contribution coming from the purely EW diagrams. The $\mathcal{O}(\alpha_s\alpha)$ QCD background processes, induced by gluon splitting diagrams, have been evaluated using the exact tree level matrix elements in the case of the EXCALIBUR and WPHACT. HZHA can evaluate these processes only in the parton shower approximation. Since this approach gives a very low generation efficiency, the results have a large statistical error. Although consistent with the exact tree level results, the EW+QCD results from HZHA have therefore not been included in the Tables.

m_H (GeV)	65	90	115	∞
CompHEP_0	37.264(58)	24.395(46)	10.696(13)	10.634(13)
$\text{CompHEP}_{4.7}$	37.147(58)	24.279(46)	10.580(13)	10.518(13)
EXCALIBUR	—	—	—	10.6398(15)
FERMISV	—	—	—	9.49(23)
GENTLE/4fan	37.3975(37)	24.4727(25)	10.7022(11)	10.6401(11)
HIGGSPV	37.393(27)	24.490(21)	10.694(16)	10.65(05)
HZHA	36.79(13)	23.53(13)	10.28(13)	10.22(13)
$\text{WPHACT}_{4.7}$	37.1634(64)	24.3245(40)	10.5863(24)	10.5243(24)
WPHACT_0	37.3990(64)	24.4727(40)	10.7027(24)	10.6407(24)
WTO	37.4099(32)	24.4765(42)	10.7036(21)	10.6416(21)

Table 2: $\sigma(e^+e^- \to \mu^+\mu^- b\bar{b})$ (fb) at $E_{cm} = 192$ GeV. No ISR.

m_H (GeV)	65	90	115	∞
CompHEP_0	64.14(15)	2.341(07)	1.279(04)	1.279(04)
$\text{CompHEP}_{4.7}$	64.12(15)	2.325(07)	1.263(04)	1.263(04)
EXCALIBUR	—	—	—	1.2916(04)
FERMISV	—	—	—	1.195(26)
GENTLE/4fan	64.2407(64)	2.36582(24)	1.29239(13)	1.29229(13)
HIGGSPV	64.199(60)	2.375(19)	1.293(09)	1.286(14)
HZHA	63.99(02)	2.258(18)	1.230(18)	1.230(18)
$\text{WPHACT}_{4.7}$	63.941(14)	2.3473(10)	1.27611(80)	1.27601(80)
WPHACT_0	64.238(14)	2.3661(10)	1.29237(82)	1.29227(82)
WTO	64.262(11)	2.36583(93)	1.29210(92)	1.2950(20)

Table 3: $\sigma(e^+e^- \to \nu_\mu\bar{\nu}_\mu b\bar{b})$ (fb) at $E_{cm} = 175$ GeV. No ISR.

m_H (GeV)	65	90	115	∞
CompHEP_0	72.64(19)	47.02(14)	19.76(08)	19.62(07)
$\text{CompHEP}_{4.7}$	72.41(19)	46.79(14)	19.53(08)	19.41(07)
EXCALIBUR	—	—	—	19.7131(40)
FERMISV	—	—	—	18.57(62)
GENTLE/4fan	72.9256(73)	47.2239(47)	19.8405(20)	19.7171(20)
HIGGSPV	72.867(63)	47.225(50)	19.786(42)	19.67(06)
HZHA	72.83(21)	46.31(21)	19.82(21)	19.71(21)
$\text{WPHACT}_{4.7}$	72.475(16)	46.944(12)	19.625(11)	19.502(10)
WPHACT_0	72.927(16)	47.222(12)	19.841(11)	19.717(11)
WTO	72.961(11)	47.2341(40)	19.8394(14)	19.7200(70)

Table 4: $\sigma(e^+e^- \to \nu_\mu \bar{\nu}_\mu b\bar{b})$ (fb) at $E_{cm} = 192$ GeV. No ISR.

m_H (GeV)	65	90	115	∞
CompHEP_0	70.26(20)	5.03(02)	1.073(04)	1.073(04)
$\text{CompHEP}_{4.7}$	70.24(20)	5.02(02)	1.059(04)	1.059(04)
EXCALIBUR	—	—	—	1.0796(03)
FERMISV	—	—	—	1.195(26)
HIGGSPV	71.727(34)	5.100(05)	1.081(01)	1.077(06)
HZHA	69.98(18)	3.572(18)	1.230(18)	1.230(18)
$\text{WPHACT}_{4.7}$	71.366(26)	5.0762(22)	1.06615(87)	1.06602(87)
WPHACT_0	71.694(27)	5.0996(23)	1.08027(89)	1.08013(89)
WTO	71.679(14)	5.0997(15)	1.07978(81)	1.0820(20)

Table 5: $\sigma(e^+e^- \to \nu_e \bar{\nu}_e b\bar{b})$ (fb) at $E_{cm} = 175$ GeV. No ISR.

m_H (GeV)	65	90	115	∞
CompHEP_0	79.01(24)	52.37(18)	20.82(08)	19.89(07)
$\text{CompHEP}_{4.7}$	78.79(24)	52.15(18)	20.60(08)	19.67(07)
EXCALIBUR	—	—	—	19.9463(44)
FERMISV	—	—	—	18.57(62)
HIGGSPV	80.628(32)	53.353(21)	20.907(13)	19.95(10)
HZHA	80.99(21)	49.80(21)	20.26(21)	19.71(21)
$\text{WPHACT}_{4.7}$	80.122(34)	53.039(19)	20.673(12)	19.736(12)
WPHACT_0	80.611(34)	53.335(19)	20.893(12)	19.955(10)
WTO	80.629(32)	53.3468(63)	20.8883(15)	19.9540(50)

Table 6: $\sigma(e^+e^- \to \nu_e\bar{\nu}_e b\bar{b})$ (fb) at $E_{cm} = 192$ GeV. No ISR.

m_H (GeV)	65	90	115	∞
EXCALIBUR	—	—	—	0.8256(04)
FERMISV	—	—	—	0.745(19)
GENTLE/4fan	28.4273(28)	1.22507(12)	0.824890(82)	0.824849(82)
HIGGSPV	28.437(14)	1.224(02)	0.8248(06)	0.817(06)
HZHA	28.317(27)	1.252(27)	0.860(27)	0.860(27)
$\text{WPHACT}_{4.7}$	28.305(17)	1.21406(85)	0.81492(81)	0.81489(81)
WPHACT_0	28.437(17)	1.22479(70)	0.82472(65)	0.82468(65)
WTO	28.456(12)	1.2241(16)	0.8232(15)	0.8232(15)

Table 7: $\sigma(e^+e^- \to \mu^+\mu^- b\bar{b})$ (fb) at $E_{cm} = 175$ GeV. ISR included.

m_H (GeV)	65	90	115	∞
EXCALIBUR	—	—	—	8.4306(29)
FERMISV	—	—	—	7.90(27)
GENTLE/4fan	33.7575(34)	19.4717(19)	8.47729(85)	8.43290(84)
HIGGSPV	33.759(12)	19.480(09)	8.483(05)	8.44(05)
HZHA	33.48(11)	18.91(11)	8.31(11)	8.27(11)
$\text{WPHACT}_{4.7}$	33.547(15)	19.3515(90)	8.3842(56)	8.3400(56)
WPHACT_0	33.752(16)	19.4692(91)	8.4767(57)	8.4324(57)
WTO	33.777(10)	19.4856(83)	8.4851(78)	8.4409(78)

Table 8: $\sigma(e^+e^- \to \mu^+\mu^- b\bar{b})$ (fb) at $E_{cm} = 192$ GeV. ISR included.

m_H (GeV)	65	90	115	∞
EXCALIBUR	—	—	—	0.9900(05)
FERMISV	—	—	—	0.928(23)
GENTLE/4fan	55.9190(56)	1.78649(18)	0.990681(99)	0.990600(10)
HIGGSPV	55.899(29)	1.786(05)	0.991(02)	0.991(12)
HZHA	55.863(14)	1.733(14)	0.949(14)	0.949(14)
$\text{WPHACT}_{4.7}$	55.644(34)	1.77146(97)	0.97777(83)	0.97770(83)
WPHACT_0	55.901(34)	1.7858(10)	0.99028(84)	0.99021(84)
WTO	55.947(27)	1.7857(14)	0.9894(13)	0.9893(13)

Table 9: $\sigma(e^+e^- \to \nu_\mu\bar{\nu}_\mu b\bar{b})$ (fb) at $E_{cm} = 175$ GeV. ISR included.

m_H (GeV)	65	90	115	∞
EXCALIBUR	—	—	—	15.5420(64)
FERMISV	—	—	—	15.14(56)
GENTLE/4fan	65.9061(66)	37.4957(37)	15.6302(16)	15.5421(16)
HIGGSPV	65.895(27)	37.504(20)	15.629(13)	15.51(06)
HZHA	65.60(14)	36.45(14)	15.25(14)	15.17(14)
$\text{WPHACT}_{4.7}$	65.500(31)	37.270(18)	15.460(12)	15.372(12)
WPHACT_0	65.894(31)	37.491(18)	15.631(12)	15.543(12)
WTO	65.922(27)	37.5201(96)	15.6356(50)	15.5474(50)

Table 10: $\sigma(e^+e^- \to \nu_\mu \bar{\nu}_\mu b\bar{b})$ (fb) at $E_{cm} = 192$ GeV. ISR included.

m_H (GeV)	65	90	115	∞
EXCALIBUR	—	—	—	0.8382(05)
FERMISV	—	—	—	0.928(23)
HIGGSPV	62.917(35)	3.903(04)	0.8398(04)	0.844(05)
HZHA	60.96(14)	2.753(14)	0.949(14)	0.949(14)
$\text{WPHACT}_{4.7}$	62.589(32)	3.8858(25)	0.82761(65)	0.82751(65)
WPHACT_0	62.876(32)	3.9037(25)	0.83849(66)	0.83838(66)
WTO	62.905(65)	3.9056(40)	0.8381(13)	0.8379(13)

Table 11: $\sigma(e^+e^- \to \nu_e \bar{\nu}_e b\bar{b})$ (fb) at $E_{cm} = 175$ GeV. ISR included.

m_H (GeV)	65	90	115	∞
EXCALIBUR	—	—	—	15.5974(69)
FERMISV	—	—	—	15.14(56)
HIGGSPV	73.051(34)	42.682(21)	16.275(12)	15.78(09)
HZHA	72.85(14)	39.35(14)	15.56(14)	15.17(14)
$\text{WPHACT}_{4.7}$	72.595(39)	42.439(20)	16.095(13)	15.418(13)
WPHACT_0	73.022(39)	42.673(20)	16.268(13)	15.590(13)
WTO	73.003(44)	42.701(17)	16.2675(58)	15.5897(58)

Table 12: $\sigma(e^+e^- \to \nu_e \bar{\nu}_e b\bar{b})$ (fb) at $E_{cm} = 192$ GeV. ISR included.

	(1)	(2)	(3)	(4)	EW	EW+QCD
EXCALIBUR	—	—	—	—	—	6.859(04)
HZHA	90.71(46)	2.902(19)	158.09(79)	4.632(54)	2.760(17)	—
WPHACT_0	—	—	—	—	2.580(2)	6.8589(87)
$\text{WPHACT}_{4.7}$	—	—	—	—	—	7.1764(84)

Table 13: $\sigma(e^+e^- \to b\bar{b}b\bar{b})$ (fb) at E_{cm} = 175 GeV. No ISR. See the text for the meaning of the labels (1) – (4). The last two columns refer to the SM background results, separated in pure EW and full EW+QCD processes.

	(1)	(2)	(3)	(4)	EW	EW+QCD
EXCALIBUR	—	—	—	—	—	25.933(10)
HZHA	135.17(61)	23.286(58)	163.36(75)	74.04(31)	22.816(50)	—
WPHACT_0	—	—	—	—	21.897(16)	25.916(18)
$\text{WPHACT}_{4.7}$	—	—	—	—	—	25.946(23)

Table 14: $\sigma(e^+e^- \to b\bar{b}b\bar{b})$ (fb) at E_{cm} = 192 GeV. No ISR. See comments in the previous figure caption.

	(1)	(2)	(3)	(4)	EW	EW+QCD
EXCALIBUR	—	—	—	—	—	8.490(20)
HZHA	76.74(39)	2.513(20)	140.20(71)	3.903(48)	2.397(18)	—
WPHACT_0	—	—	—	—	2.239(2)	8.447(22)
$\text{WPHACT}_{4.7}$	—	—	—	—	—	8.993(21)

Table 15: $\sigma(e^+e^- \to b\bar{b}b\bar{b})$ (fb) at E_{cm} = 175 GeV. ISR included. See previous figure caption for comments.

	(1)	(2)	(3)	(4)	EW	EW+QCD
EXCALIBUR	—	—	—	—	—	23.045(23)
HZHA	118.60(58)	18.761(87)	151.75(75)	57.74(28)	18.384(80)	—
WPHACT_0	—	—	—	—	17.482(14)	22.991(34)
$\text{WPHACT}_{4.7}$	—	—	—	—	—	23.258(37)

Table 16: $\sigma(e^+e^- \to b\bar{b}b\bar{b})$ (fb) at E_{cm} = 192 GeV. ISR included. See previous figure caption for comments.

3 Supersymmetry

Supersymmetry [28] is considered to be the most likely candidate for new physics within the reach of LEP2 [5]. We assume here that the reader is familiar with the basics of SUSY and with its most common parameters, and we refer to the review articles in ref. [28] or to the New Physics report [5] for definitions and details. A large body of work has been devoted in the past 10 years to the development of event generators for the simulation of SUSY signals. Due to the large interest in the subject, the number of computer programs which calculate cross sections or generate events is very large; however most of these codes have not been designed for distribution, and are not documented here. We will limit ourselves to present codes which have either been developed during the Workshop, or which have been discussed and used within the activity of the New Physics Working group. All of these codes are either already public, or will soon become.

The main difference between SUSY generators for LEP1 and for LEP2 is related to the significant rôle played at LEP2 by t-channel exchange diagrams, which are almost totally negligible at the Z peak. As a typical example, consider the chargino pair production. This can proceed via s-channel γ-Z production, or via t-channel exchange of the electron scalar-neutrino ($\tilde{\nu}_{ee}$). The interference is always destructive, and can significantly reduce the production cross section if the sneutrino mass is in the 50–100 GeV region. Another example, documented in the New Physics section of this report [5], is that of the scalar electron production, where the t-channel exchange of a neutralino can either decrease or increase the rates.

Alhtough documented only in part in this report, extensive cross checks among the different codes used by the experimental groups have been performed. These checks included the study of the proper inclusion of t-channel diagrams, of the dependence of cross sections on the parameters of the models, as well as studies of kinematical distributions and of the effects of the initial state radiation (ISR). Comparisons of decay branching ratios(BR) for unstable particles have also been performed. All tests have been pursued until agreement at the percent level was achieved.

In most SUSY generators, the emphasis is placed on covering as many processes as possible

in a unified framework. By doing so, the simplest approaches have often been pursued. For example, it is generally assumed that production and decay of SUSY states can be factorized, therefore neglecting possible initial–final state spin correlations. This choice is forced upon us by the multitude of possible decays which each SUSY particle has allowed as soon as the parameters of the theory are slightly changed. Each decay channel would in principle call for a new evaluation of matrix elements with many-body final states, including the interference with SM processes and possibly with other SUSY channels. The multitude of channels to be considered for a generic point in parameter space is such that a thorough evaluation of the full matrix elements for all SUSY particles has never been carried out, and finds no place in any multi-purpose SUSY event generator. In order to assess the limit of this approach, several groups have started working on more specific channels, where the structure of the final state is better determined and where full calculations can be performed and compared to the simpler results. We will report here on one such development, namely the construction of an event generator for chargino production and decay which is based on the evaluation of the full matrix elements.

Another important feature of SUSY event generators is the possibility to impose or relax sets of assumptions or constraints on the parameters of the model. Several theoretical frameworks (*e.g.* Minimal Supergravity) predict relations between some of free SUSY parameters, and allow to produce more specific predictions than otherwise possible. At the same time, it is however important to be able to free themselves from relations which could artificially constrain rates or properties of a given process, in order to make the experimental searches as unbiased as possible. The following documentation will describe to which extent the available codes provide such handles.

3.1 SUSYGEN

Program name:	SUSYGEN
Authors:	S. Katsanevas – `katsanevas@vxcern.cern.ch`
	S. Melachroinos – `melachr@vxcern.cern.ch`
Availability:	`vxcern::disk$delphi:[katsanevas.susygen]`
	Files `susygen.for` and `susygen.com`
Documentation:	vxcern::disk$delphi:[katsanevas.susygen]susygen_manual.ps

SUSYGEN is a Monte Carlo generator for the production and decay of all (R-Parity odd) MSSM sparticles in e^+e^- colliders. It is flexible enough that the user can assume or relax different theoretical constraints, and it is easily generalizable to extensions of the MSSM such as the Next to Minimal Supersymmetric Standard Model (NMSSM) or R-Parity violating processes [2]. In particular, R-Parity violating decays [33] of the $\tilde{\chi}_1^0$ (assumed to be the lightest supersymmetric particle) can be selected by the user through data cards. Each of the possible

[2]The parts of the code relative to Higgs and radiative decays of neutralinos and charginos were kindly provided by S. Ambrosanio. Those relative to R-Parity violation interactions by H. Dreiner.

45 R-parity violating operators described in the New Physics Chapter of this Report is allowed. The input parameters specifying the SUSY model are chosen to be:

1. m_0, the common mass of the spin 0 squarks and sleptons, at the GUT scale.
2. M_2, the SU(2) gaugino mass parameter at the EW scale.
3. μ, the mixing parameter of the Higgs doublets at the EW scale,
4. $\tan\beta$, the ratio of the vacuum expectation values of the two Higgs doublets.
5. A, the trilinear coupling in the Higgs sector. This is used only for the calculation of the third generation mixing.
6. and m_A, the mass of the pseudoscal Higgs. This is used only for the calculation of the Higgs spectrum.

Initial state radiation and an interface to JETSET [16] are included.

The production and decay matrix elements are taken from ref. [31]. Direct production of R-even MSSM particles, namely the neutral and charged Higgs bosons h, H, A and $H^{\pm}$, will be included in the next version of the program.

Production and decay of unstable SUSY particles are factorized, and therefore full initial/final state spin correlations are not included. Nevertheless 2- and 3-body decays are generated using the complete matrix elements, including contributions from all possible bosonic and fermionic intermediate states. Decays to Higgs bosons and radiative decays of neutralinos and charginos are included as well [32]. Since all unstable SUSY particles are decayed before the call to JETSET, $\tilde{t}$ hadronization is not included.

SUSYGEN has been tested extensively and found to agree within 1% with ISAJET (see next Section) in what concerns the production cross sections, and to agree with the production and decay branching ratios generated by the code of the authors of ref. [32]. The code and complete documentation, including a detailed list of cross section formulae and sample outputs from the code, can be found in `vxcern::disk$delphi:[katsanevas.susygen]` in the files `susygen.for, susygen.com` and `susygen_manual.ps`.

Decays Some detail on the treatment of SUSY particle decays in SUSYGEN is given here. For the decays of the $\tilde{\chi}^0$'s and $\tilde{\chi}^{\pm}$'s one can in general distinguish two regimes. If all scalar masses are very large, or the fermions are mostly gauginos, the decay occurs through an off-shell W or Z boson, *e.g.* $\tilde{\chi}_1^{\pm} \to W^{*\pm}\tilde{\chi}_1^0$ or $\tilde{\chi}_2^0 \to Z^*\tilde{\chi}_1^0$ and $\tilde{\chi}_2^0 \to W^{\mp}\tilde{\chi}_1^{\pm}$. In this case the BR's to the different final state leptons or quarks are mostly determined from those of the off-shell Z and W. If instead the SUSY fermions are mostly charginos, and some scalar lepton and/or quark has mass comparable to the masses of W and Z, decays mediated by the virtual scalars can dominate, and the BR's to the corresponding fermions can be enhanced. Since it is assumed that $\tilde{\chi}_1^0$ is the LSP, only two-body prompt decays of scalar particles are considered. Should

other charginos or neutralinos be lighter than a given scalar, cascade decays through them are included.

SUSYGEN does not distinguish between three-body and two-body decays (when e.g the decay to an on-shell scalar is posssible) since it includes the widths of the scalars in the propagators and therefore lets the propagators force the two-body kinematics, including all possible interferences. There is a small region where the decays to Higgses or the radiative decays dominate: these rare decays are included in the list of possible decays. They can be studied separately by setting the other branching ratios to zero through the data card DECSEL. The masses of the Higgses are calculated by using two-loop evolution equations [14].

Program structure. SUSYGEN is divided in three stages. In the first stage the subroutine SCARDS reads the steering cards and the subroutine SBOOK books some standard histograms. The standard histograms in the case of the SCAN option are: the masses, cross-sections and decay branching ratios in 2-d histograms of μ versus M. In the case of the no-SCAN option, the cosθ distribution of the produced objects are reproduced.

In the second stage the routine SUSANA initializes the masses and the branching ratios of MSSM sparticles. The masses of sleptons and squarks are evaluated by assuming a common m_0 mass at GUT unification and running it down to electroweak scales through Renormalization Group Equations (RGE's). Chargino and neutralino masses and mixings are evaluated through the diagonalization of the gaugino and Higgsino mass matrices [31].

The double differential cross sections $\frac{d\sigma}{dsdt}$ have been integrated analytically over t, and then integrated numerically over s inside the subroutine BRANCH. Subroutine INTERF stores the results for further generation. Particle codes are assigned by default their LUND values, while the naming used by ISAJET 7.03 [34] has been retained for comparison purposes.

The third stage calculates the cross sections and generates the sparticles requested by the user via data cards. The cross sections are computed from the functions: CHARGI (production cross section for $\tilde{\chi}^{\pm}$), PHOTI (production cross section for all $\tilde{\chi}^0$), GENSEL (production cross section for $\tilde{e}$), GENSELR (production cross sections for $\tilde{e_L}, \tilde{e_R}$), GENSMUS (production cross section for $\tilde{\mu}, \tilde{\tau}, \tilde{q}$), GENSNUE (production cross section for $\tilde{\nu}_{ee}$), GENSNU (production cross section for $\tilde{\nu}_e$). The user can also select through cards the luminosity available, so after this stage the number of events to be generated is calculated.

Unweigthed events generated according to the appropriate cos θ distribution are produced by the routine SUSYEVE. Subroutine DECABR using the tabulated branching ratios determines the branching ratio of the decay. SMBOD2 and SMBOD3 generate the 4-vectors of the decay products at each decay vertex. The program loops till DECABR indicates there is no other possible decay. When the RPARITY card is TRUE the above condition is fulfilled when we have the lowest lying neutralino and standard particles in the products. When RPARITY is FALSE routine LSPDECAY is called and the neutralino decays to the prescribed standard particles. The above 4-vectors are interfaced to LUND in subroutine SFRAGMENT where they fragment and decay.

The last subroutines of MSSMGENE are SXWRLU which writes the LUND common block to an external file (unit 12) and a small routine USER gives access to the LUND common after generation. The subroutine SUSEND closes the program, and stores the standard histograms to the file SUSYGEN.HIST. SUSYGEN uses routines from the libraries `jetset74, packlib` and `genlib` and it has therefore to be linked to them.

3.2 ISAJET

Program name:	ISAJET 7.16
Authors:	H. Baer – `baer@fsuhep.physics.fsu.edu`
	F. Paige, `paige@bnlux1.bnl.gov"`
	S. Protopopescu `serban@bnlux1.bnl.gov"`
	X. Tata `tata@uhhepj.phys.hawaii.edu"`
Availability:	Patchy source file via anonymous ftp from
	`bnlux1.bnl.gov:pub/isajet.`
	Files: `isajet.car, makefile.unix` (UNIX) and `isamake.com` (VMS)
Documentation:	ISAJET.DOC can be extracted from isajet.car
	via makefile.unix or isamake.com

The program ISAJET [34], originally developed to generate events for hadron colliders, can also be used for event generation at e^+e^- machines. In particular, the latest version, ISAJET 7.15, contains the following SM $2 \to 2$ subprocesses

$$\begin{aligned} e^+e^- &\to f\bar{f}, \\ e^+e^- &\to WW, \\ e^+e^- &\to ZZ, \end{aligned}$$

where $f = e, \mu, \tau, \nu_e, \nu_\mu, \nu_\tau, u, d, s, c, b$ and t. ISAJET includes the Fox-Wolfram final state shower QCD radiation [35] and Field-Feynman hadronization [36]. Spin correlations for the $e^+e^- \to WW$ and ZZ processes are currently neglected, as is initial state photon radiation. ISAJET 7.15 does contain the capability to generate events assuming longitudinally polarized e^+ or e^- beams, although this option may mainly be of interest to linear e^+e^- collider enthusiasts.

ISAJET also contains a large amount of code relevant for Supersymmetry. Currently, one may input into ISAJET either MSSMi or SUGRA keywords, corresponding to two different parameter sets. For MSSM parameters, the inputs are:

$$\begin{aligned} MSSM1: &\quad m_{\tilde{g}},\ m_{\tilde{q}},\ m_{\tilde{\ell}_L},\ m_{\tilde{\ell}_R},\ m_{\tilde{\nu}}, \\ MSSM2: &\quad m_{\tilde{t}_L},\ m_{\tilde{t}_R},\ A_t,\ m_{\tilde{b}_R},\ A_b, \\ MSSM3: &\quad \tan\beta,\ \mu,\ m_A. \end{aligned}$$

The various sparticle masses and mixings are then calculated, as well as sparticle decay modes and branching fractions. GUT scale gaugino mass unification is assumed, as is the degeneracy of the first two generations of squarks, and the first three generations of sleptons (although intra-generational slepton splitting is maintained). A complete set of Higgs boson mass and coupling radiative corrections (evaluated in the one-loop effective potential) are included, as well as all Higgs decay modes to particles and sparticles [37]. An independent program ISASUSY can be extracted from ISAJET which yields a hard copy of the various sparticle masses, parameters and decay branching fractions.

ISAJET also can generate a sparticle spectrum given the parameter set of the minimal supergravity (SUGRA) GUT model with radiative electroweak symmetry breaking [38]. In this case, the input parameters are:

$$SUGRA:\ m_0,\ m_{1/2},\ A_0,\ \tan\beta,\ sgn(\mu).$$

The top mass m_t also needs to be specified. ISAJET will then calculate sparticle masses by evolving 26 renormalization group equations between the weak scale and GUT scale, in an iterative procedure, using Runge-Kutta method. Gauge coupling unification is imposed, but not Yukawa unification. Weak scale sparticle threshold effects are included in the gauge coupling evolution. Two loop RGE's are used for gauge and Yukawa evolution, while one-loop RGE's are used for the other soft-breaking parameters. In the end, radiative electroweak symmetry breaking is imposed, using the one-loop corrected effective potential. A full set of radiative corrections are included for the Higgs boson masses and couplings. In addition, the running gluino mass is converted to a pole gluino mass. An independent program ISASUGRA can be extracted from ISAJET which yields a hard copy of the resultant sparticle masses, parameters and decay branching fractions.

All lowest order $2 \to 2$ sparticle and Higgs boson production mechanisms have been incorporated into ISAJET. These include the following processes [39] (neglecting bars over anti-particles):

$$\begin{aligned}
e^+e^- &\to \tilde{q}_L\tilde{q}_L,\ \tilde{q}_R\tilde{q}_R,\\
e^+e^- &\to \tilde{\ell}_L\tilde{\ell}_L,\ \tilde{\ell}_R\tilde{\ell}_R,\ \tilde{e}_L\tilde{e}_R,\\
e^+e^- &\to \tilde{\nu}_\ell\tilde{\nu}_\ell,\\
e^+e^- &\to \tilde{\chi}_1^\pm\tilde{\chi}_1^\mp,\ \tilde{\chi}_2^\pm\tilde{\chi}_2^\mp,\ \tilde{\chi}_1^\pm\tilde{\chi}_2^\mp,\\
e^+e^- &\to \tilde{\chi}_i^0\tilde{\chi}_j^0,\ (i,j=1-4),\\
e^+e^- &\to Zh,\ ZH,\ Ah,\ AH,\ H^+H^-.
\end{aligned}$$

In the above, $\ell = e,\ \mu$ or τ. All squarks (and also all sleptons other than staus) are taken to be L or R eigenstates, except the stops, for which $\tilde{t}_1\tilde{t}_1$, $\tilde{t}_1\tilde{t}_2$ and $\tilde{t}_2\tilde{t}_2$ (here, $\tilde{t}_{1,2}$ being the lighter/heavier of the top squark mass eigenstates) production is included.

Given a point in SUGRA or MSSM space, and a collider energy, ISAJET generates all allowed production processes, according to their relative cross sections. The produced sparticles

or Higgs bosons are then decayed into all kinematically accessible channels, with branching fractions calculated within ISAJET. The sparticle decay cascade terminates with the lightest SUSY particle (LSP), taken to be the lightest neutralino ($\tilde{\chi}_1^0$). ISAJET currently neglects spin correlations and sparticle decay matrix elements. In the above reactions, spin correlation effects are only important for chargino and neutralino pair production, while decay matrix elements are mainly important for 3-body sparticle decays. ISAJET 7.15 also includes capability to generate SUSY and Higgs processes with polarized beams. Sample results from running ISAJET for LEP2 are given in Ref. [40].

The complete card image PAM file for ISAJET 7.15 can be copied across HEPNET, the high energy physics DECNET, from bnlcl6::2dua14:[isajet.isalibrary]isajet.car. A Unix makefile makefile.unix and a VMS isamake.com are available in the same directory. The same files can be obtained by anonymous ftp from bnlux1.bnl.gov:pub/isajet.

A sample input file for generating all sparticle processes at LEP2 is given below:

```
SAMPLE LEP2 SUGRA JOB
175.,100,0,0/
E+E-
NTRIES
2000/
SEED
999999999956781/
TMASS
180,-1,1/
SUGRA
100,80,0,2,-1/
JETTYPE1
'ALL'/
JETTYPE2
'ALL'/
END
STOP
```

3.3 SUSYXS

Program name:	SUSYXS 1.0, Dec 15 1995
Authors:	M. Mangano – `mlm@vxcern.cern.ch`
	G. Ridolfi – `ridolfi@vxcern.cern.ch`
Availability:	`http://www.ge.infn.it/LEP2` and
	`http://surya11.cern.ch/users/mlm/SUSY`
Documentation:	To be found in the above WWW directories

This is not an event generator, but a collection of simple programs to evaluate total cross sections for SUSY particles in e^+e^- collisions. No decays nor evaluation of decay BR's are included. This set of programs is mostly useful as a reference, to obtain quickly total production rates as a function of the various relevant parameters. It was used during the workshop as a benchmark for the comparisons among the different codes. The following processes are available (each encoded in a different fortran program):

- chargino pair production (`chargino.for`).
  Input parameters: $\sqrt{s}$, M_2, μ, $\tan\beta$, $M(\tilde{\nu}_{ee})$.
- neutralino pair production, for all possible neutralino pairs (`neutralino.for`).
  Input parameters: $\sqrt{s}$, M_2, μ, $\tan\beta$, $M(\tilde{e})$.
- selectron pair production (LL, RR and RL) (`selectron.for`).
  Input parameters: $\sqrt{s}$, $M(\tilde{e}_L)$, $M(\tilde{e}_R)$, M_2, μ, $\tan\beta$,
- smuon pair production (LL, RR) (`smuon.for`).
  Input parameters: $\sqrt{s}$, $M(\tilde{\mu}_L)$, $M(\tilde{\mu}_R)$.
- stop pair production (`stop.for`).
  Input parameters: $\sqrt{s}$, $M(\tilde{t}_1)$, $M(\tilde{t}_2)$, θ_{LR}.
- Higgs production (`higgs.for`).
  Input parameters: $\sqrt{s}$, M_A, $\tan\beta$, $M(\tilde{q})$.

ISR is included, as well as QCD corrections in the case of stop production [29]. All references for the formulas used are included as comments in the fortran files. The Higgs production code includes the one-loop-corrected masses [1], using the formulas of ref. [30].

How the code works. The code relative to the process of interest has to be linked to `phoisr` (which incorporates the ISR corrections) and to the CERN libraries. The executable can be run interactively, and the input parameters can be entered by the user at running time. Results with and without ISR are printed. In the case of chargino, neutralino and higgs production, the mass spectra are given as well. The codes are simple enough that any user can modify them easily to customize the output and produce directly, for example, cross section distributions or scatter plots. Likewise, the extraction of angular distributions for most processes is straightforward, as all needed formulas are collected in the codes.

3.4 SUSY23

Program name:	SUSY23 version 1.0
Authors:	J. Fujimoto, T. Ishikawa, M. Jimbo, T. Kaneko, K. Kato, S. Kawabata, T. Kon, Y. Kurihara, D. Perret-Gallix, Y. Shimizu, H. Tanaka `susy23@minami.kek.jp`
Availability:	Anonymous ftp: `ftp.kek.jp` Files in: `/kek/minami/susy23`.
Documentation:	

This is a Monte-Carlo unit-weight event generator for $2 \to 3$ SUSY processes at LEP2 energies, based on the minimal supersymmetric standard model (MSSM.).

Features of the program:

- Processes available: $e^+e^- \to \chi_1^+\chi_1^-$, $\tilde{\ell}_{L,R}^+\tilde{\ell}_{L,R}^-$, $\tilde{\nu}_\ell^*\tilde{\nu}_\ell$, $\tilde{t}_1^*\tilde{t}_1$, $\tilde{b}_1^*\tilde{b}_1$, $\chi_1^0\chi_2^0$, $\chi_2^0\chi_2^0$, $\gamma\chi_1^0\chi_1^0$, $e^\pm\tilde{e}^\mp\chi_1^0$, $e^\pm\tilde{\nu}\chi_1^\mp$
- Initial state radiation implemented using the structure function approach, and using QEDPS in some processes [41]
- Final sparticle decays included (see below)
- Hadronization realized via an interface with JETSET [16].

How the code works. FORTRAN source codes are generated by **GRACE** [42] which is a program for automatic computation of Feynman amplitudes. Largely exercised on standard model processes, **GRACE** is being used in the SUSY framework thanks to the addition of a dedicated vertex and propagator library. Tools have been developed to build automatically the SUSY23 event generator from the various processes thus prepared. Based on an open architecture, the generator can easily accommodate the addition of foreseen more complex processes ($2 \to 4$). The numerical integration of the differential cross section over the phase space is carried out by the program BASES[7]. All information on the event kinematics and the phase space hyper-cell weight map are then used by the event generation program SPRING[7] to produce unit-weight events.

Helicity informations are available at the parton level. The hadronization is performed through the interface to the JETSET [16] package which has been extended to incorporate SUSY particle codes.

In this version (V1.0), the user may generate only one process per run, in future releases, the possibility will be given to produce events from a selected set of processes accordingly to their respective probability.

Input parameters Two approaches have been developed to better suit the user needs:

- A general program contains all process codes, the selection being performed by setting data cards.
- An interactive tool using menus and requesters gives the user the possibility to build a generator dedicated to a single process.

The following parameters can be set by the user:

- Selection of SUSY processes
- Center of mass energy : $\sqrt{s}$
- Experimental cuts
  - angle cuts for each sparticles
  - energy cuts for each sparticles
  - invariant mass cuts
- SUSY parameters

The program is based on the MSSM and the notation for SUSY parameters in ref. [43] is adopted. The input SUSY parameters are:

- gaugino parameters: $\tan\beta$, M_2, μ
- scalar lepton masses: $m_{\tilde{\ell}_L}$, $m_{\tilde{\ell}_R}$
- scalar (light) quark masses: $m_{\tilde{q}_L}$, $m_{\tilde{q}_R}$
- third generation scalar quark masses: $m_{\tilde{t}_1}$, $m_{\tilde{t}_2}$, θ_t, $m_{\tilde{b}_1}$, $m_{\tilde{b}_2}$, θ_b

General GRACE parameters can be found in the GRACE manual [42] (Helicity amplitude techniques, diagram generation and selection, phase space integration, event generation).

Sparticle decays. Particle widths and decay branching ratios for all possible modes are calculated. Each event final state is then generated according to these probabilities. We have included some possible cascade decays of sparticles as well as 2-body and 3-body direct decays.

Check of results We compared the results for 2-body processes, $e^+e^- \to \chi_1^+\chi_1^-$, $\tilde{\ell}_{L,R}^+\tilde{\ell}_{L,R}^-$, $\tilde{\bar{\nu}}_\ell\tilde{\nu}_\ell$, $\tilde{\bar{t}}_1\tilde{t}_1$, $\tilde{\bar{b}}_1\tilde{b}_1$, $\chi_1^0\chi_2^0$, $\chi_2^0\chi_2^0$ with the analytical exact calculation. As for the 3-body processes, $e^+e^- \to e^\pm\tilde{e}^\mp\chi_1^0$, $e^\pm\tilde{\nu}\chi_1^\mp$, the results were checked against the analytical calculation based on the equivalent photon approximation. For the radiative process, $e^+e^- \to \gamma\chi_1^0\chi_1^0$, we compared the result with the exact calculation for $e^+e^- \to \gamma\tilde{\gamma}\tilde{\gamma}$ by taking a specific parameter points which corresponds to the case $\chi_1^0 \simeq \tilde{\gamma}$. The results for all 2-body processes are consistent with those of SUSYGEN [48].

3.5 DFGT: a chargino MC generator with full spin correlations

Program name: DFGT
Authors: C. Dionisi – dionisi@vxrm70.roma1.infn.it
K. Fujii – fujiik@jlcux1.kek.jp
S. Giagu – giagu@vxcern.cern.ch
T. Tsukamoto – tsukamot@kekvax.kek.jp

Availability:
Documentation:

General features. We shortly summarize the features and performances of a new Montecarlo event generator, DFGT [45] which takes properly into account the full spin correlations that occur in the amplitude due to the matching of the spin of the produced and the decaying particle. The choice of SUSY parameters is that of the minimal supergravity scenario, assuming the GUT-relations [43]. The masses and the couplings of the SUSY particles are then specified by the four parameters m_0, M_2, μ and $\tan\beta$.

The events are generated as follows:

- Full helicity amplitudes including decays into final state partons are first calculated at tree level. This is done using HELAS library routines [46], which allows to implement correct angular correlations and effects of the natural widths of unstable partons.
- The effective cross sections are then evaluated by the numerical integration package BASES [7]. Initial state radiation is included in the structure function formalism, using the results of ref. [47].
- The generation of unweighted events is done at the partonic level using the SPRING package [7], and the QCD evolution and hadronization of the final state quarks in performed via an interface with JETSET 7.4 [16].

Chargino pair production takes place via s-channel γ and Z^0 exchange and via t-channel $\tilde{\nu}$ exchange. Only the light chargino and the lightest neutralino (taken as the LSP) are currently described by DFGT . Furthermore, it is assumed that charginos are lighter than all sfermions. The case of a $\tilde{\nu}$ lighter than the chargino [44], the dominant decay mode being then $\tilde{\chi}_1^{\pm} \to \tilde{\nu} l^{\pm}$, will be described in a forthcoming paper [45].

DFGT performance and comparison with SUSYGEN. Some results from the DFGT Montecarlo will now be presented. Figure 1(a) gives the total cross section of the chargino pair production as a function of $m_{\tilde{\nu}}$ showing the well known behaviour due to the interference between the s-channel and the t-channel amplitudes. The total cross sections at $\sqrt{s} = 190$ GeV with and without ISR corrections, and the total chargino widths for six points of the SUSY parameter space are listed in table 17. The six points, all with $\tan\beta = 1.5$, correspond to the the following set of parameter values:

1. $\mu = -190$ GeV, $M_2 = 65$ GeV
2. $\mu = -180$ GeV, $M_2 = 150$ GeV
3. $\mu = -40$ GeV, $M_2 = 240$ GeV

Labels A and B in table 17 correspond to $m_0 = 1000$ GeV and $m_0 = 90$ GeV, respectively.

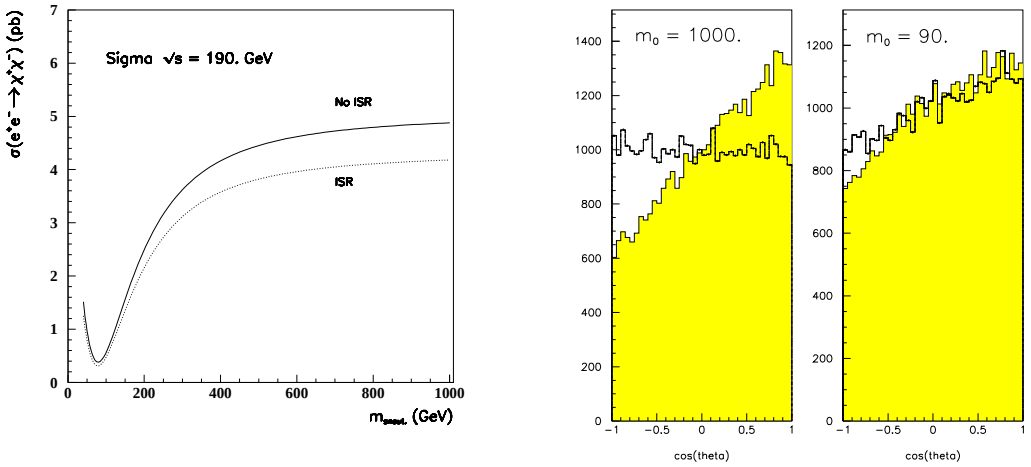

(a) (b)

Figure 1: (a) Total cross section for chargino pair production as function of $m_{\tilde{\nu}}$and (b) angular distributions for the fermions for the set 1A and 1B (Filled histogram: DFGT and histogram+dots: SUSYGEN).

For comparison the cross sections from SUSYXS (see section 3.3) and the total widths from SUSYGEN are also given. The cross sections agree at the percent level, while for the widths the agreement is of the order of few percent.

The effect of the spin correlations will now be shown by comparing some key distributions from DFGT and SUSYGEN at the generator level.

The angular distributions of the final state fermions for the parameter set 1A (which gives $m_{\tilde{\chi}^{\pm}} = 86$ GeV, $m_{\tilde{\chi}^0} = 37$ GeV, $m_{\tilde{l}} \simeq m_{\tilde{q}} \simeq 1000$ GeV) are shown in fig. 1 (a). Here θ is the angle between the outgoing fermion and the incoming electron. It is worth noticing that because of the large value of $m_{\tilde{\nu}}$ chargino production is dominated by the s-channel contribution, with the decay mode being dominated by $\tilde{\chi}_1^{\pm} \to W^* \tilde{\chi}^0 \to f \bar{f}' \tilde{\chi}^0$. The peak at $\cos\theta = 1$ is entirely due to the spin correlations, and is completely absent in the SUSYGEN distribution.

Set	$\Gamma_{\tilde{\chi}^{\pm}}$ (keV)		σ (pb)	
	DFGT	SUSYGEN	DFGT	SUSYXS
1A	37.69	37.58	4.849 (born)	4.849 (born)
			4.150 (ISR)	4.144 (ISR)
1B	66.77	66.79	0.538 (born)	0.532 (born)
			0.452 (ISR)	0.449 (ISR)
2A	35.80	36.87	3.630 (born)	3.623 (born)
			3.090 (ISR)	3.038 (ISR)
2B	39.07	40.21	1.656 (born)	1.659 (born)
			1.415 (ISR)	1.419 (ISR)
3A	2.79	2.75	3.503 (born)	3.551 (born)
			3.605 (ISR)	3.640 (ISR)
3B	2.79	2.75	3.287 (born)	3.324 (born)
			3.393 (ISR)	3.419 (ISR)

Table 17: Cross sections and total chargino widths for six points of SUSY parameter space.

The same distributions for the set 1B are given in 1 (b). Contrary to case 1A, now the t-channel contribution to the production and the $\tilde{\chi}_1^{\pm} \to \tilde{f}^* \nu \to f \bar{f}' \chi 0$ decay are relevant. Although less pronounced than in DFGT , the forward peak in the distribution appears now also in the SUSYGEN case. This reflects the non-trivial chargino angular distribution induced by the t-channel diagram. More work trying to pin down in detail how spin correlations affect the angular distributions is under way [45].

The impact of these differences on the chargino search has been checked by comparing at the generator level the distributions which play a major rôle in separating the signal from the physics backgrounds. Figs. 2 and 3 show, for DFGT and SUSYGEN , the missing p_T, the visible energy, the missing mass and the fermion-momentum distributions for set 1B (for set 1A the agreement is very good and it is not shown here). Although there is a systematic shift of about 1 GeV between the mean values for all the distributions, there is a good agreement in the tails in the regions where the cuts are applied. The importance of such effects has also been evaluated through a complete analysis of the two generators and using a full L3 detector simulation. The two analysis give essentially the same results for the sets of parameters considered here. However it is important to point out that in other points of the SUSY parameter space the conclusion might be different, in particular in regions where the mass splitting between the chargino and the neutralino is small, and where both are Higgsino-like. These cases are currently under investigation [45].

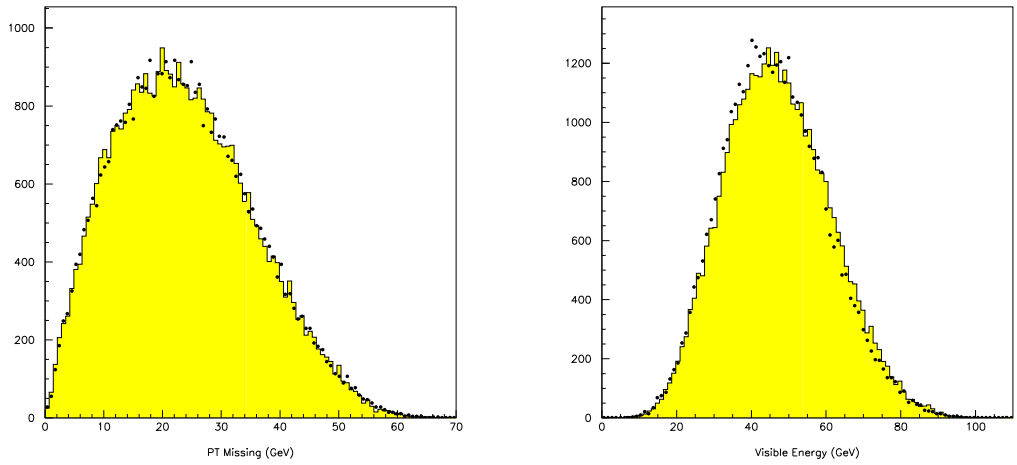

(a) (b)

Figure 2: Missing p_T(a) and Visible Energy (b) distributions, for DFGT (histogram) and SUSYGEN (dots).

3.6 Scalar top and scalar bottom event generators

The top quark has two supersymmetric partners, $\tilde{t}_L$ and $\tilde{t}_R$. The mass eigenstates, $\tilde{t}_1$ and $\tilde{t}_2$, are mixtures of the two given by the mixing angle θ_{LR}. In this section we briefly describe and compare the generators developed by different LEP experiments for the production and decay of $\tilde{t}_1$ (from now on simply indicated by $\tilde{t}$) pairs. As discussed in detail ref. [5], the cross section and kinematics of the $\tilde{t}$ production is governed by two free parameters, the stop mass $m_{\tilde{t}}$ and θ_{LR}. The only decay channels which are of potential interest at LEP2 are $\tilde{t} \to \tilde{\chi}_1^0 c$ and $\tilde{t} \to \tilde{\chi}_1^+ b$. The latter decay channel has unit branching ratio when kinematically allowed; otherwise, the dominant final state becomes $\tilde{\chi}_1^0 c$. The decay mode is therefore completely specified by stop, chargino and neutralino masses. The chargino then decays via $\tilde{\chi}_1^+ \to W^{+*}\tilde{\chi}_1^0 \to f\bar{f}'\tilde{\chi}_1^0$; the decay into a real W^+ is almost always forbidden in the LEP2 energy range. The relative values of the stop, neutralino and chargino masses are the most significant parameters for the determination of the detection efficiencies.

The two most significant issues in the development of an event generator for $\tilde{t}$ are the treatment of the perturbative radiation off the $\tilde{t}$, and of the $\tilde{t}$'s hadronization and decay. Since the $\tilde{t}$ is a scalar particle, the spectrum of gluons emitted during the perturbative evolution will differ from that of a quark. Therefore the standard shower evolution codes such as JETSET would in principle require modifications in order to incorporate the correct radiation off the $\tilde{t}$. The Altarelli-Parisi splitting function describing the $\tilde{t} \to \tilde{t}g$ branching as a function of the

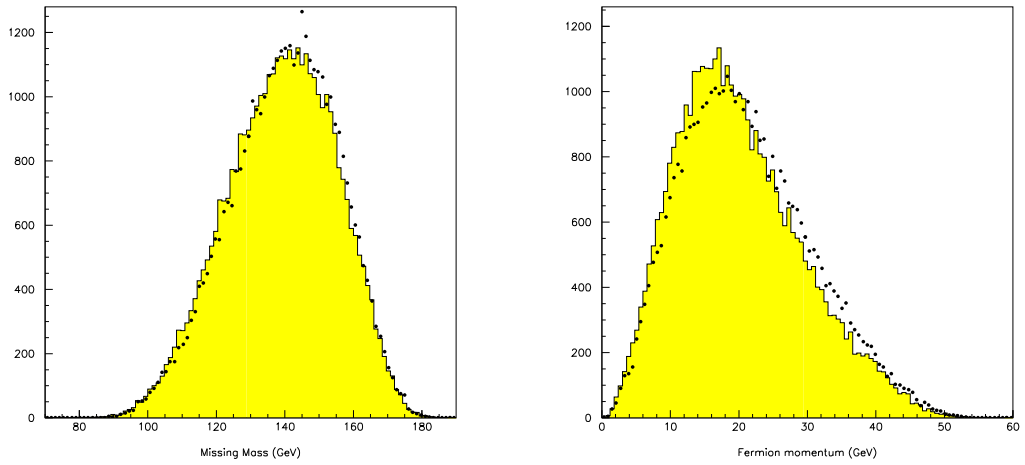

(a) (b)

Figure 3: Missing Mass (a) and Fermion Momentum (b) distributions, for DFGT (histogram) and SUSYGEN (dots).

fractional energy carried away by the gluon ($x_g = 1 - x_q$) is given by:

$$P_{\tilde{q}\tilde{q}}(x_q) = \frac{\alpha_s C_F}{2\pi}\left[\left(\frac{1+x_q^2}{1-x_q}\right)_+ - (1-x_q)\right] \tag{3.1}$$

with $C_F = 4/3$, to be compared to the standard spin-1/2 case:

$$P_{qq}(x_q) = \frac{\alpha_s C_F}{2\pi}\left(\frac{1+x_q^2}{1-x_q}\right)_+ \tag{3.2}$$

Notice that $P_{qq}(x) > P_{\tilde{q}\tilde{q}}(x)$, namely the $\tilde{t}$ fragmentation function will be harder than that of a fermion of the same mass. Notice however that the difference is proportional to the gluon energy, and vanishes in the soft gluon limit ($x_q \to 1$). Therefore it can be consistently neglected within the approximations used by most shower Monte Carlo programs. More quantitatively, one can estimate the average energy loss due to perturbative gluon emission from a particle of mass m using the well known expression [49]:

$$\langle x_g \rangle = 1 - \left[\frac{\alpha_s(m)}{\alpha_s(E)}\right]^{P^{(2)}/(2\pi b)}, \tag{3.3}$$

where $P^{(2)}$ is the second moment of the relevant splitting function, $b = (33 - 2N_f)/(12\pi)$ and E is the beam energy. Using the values of $P^{(2)} = -C_F$ for a spin-0 particle and $-4/3C_F$ for

spin-1/2, it is easy to find:

$$\langle x_g \rangle_0 - \langle x_g \rangle_{1/2} = \frac{\alpha_s(E) C_F}{3\pi} \log \frac{E}{m} \tag{3.4}$$

At 190 GeV, this difference ranges between 0.01 and 3×10^{-3} for $45 < m_{\tilde{t}} < 80$ GeV, with average energy losses for the scalar case of 3% and 1%, respectively. Such effects are totally negligible.

As for the issue of $\tilde{t}$ hadronization, it is important to realize that when the dominant decay mode is $\tilde{t} \to \tilde{\chi}_1^0 c$ the $\tilde{t}$ lifetime is longer than the typical time scale of hadron formation, and $\tilde{t}$-hadrons are formed before decay. Therefore, $\tilde{t}$ hadronization must be taken into account by Monte Carlo generator. This has been done within different approaches, which will be described and compared in the following.

Improvements and extentions of the existing codes, in order to achieve a more precise description of $\tilde{t}$ physics, are possible and foreseen. For details on the individual generators, see [50, 51, 52].

3.6.1 The DELPHI event generator.

The DELPHI $\tilde{t}$ and $\tilde{b}_1$ event generators are based on the packages BASES and SPRING [7], which perform the multidimensional phase space integration and the event unweighting. The expression of the differential production cross section for $\tilde{t}$ and $\tilde{b}_1$ pairs has been computed using the results of ref. [29], which include initial state QED radiation in the collinear approximation at the leading order, and QCD corrections.

The event generator has been interfaced with JETSET 7.3 [16] in order to completely describe the evolution and hadronization of the colored partons. Perturbative gluon radiation off the $\tilde{t}$ is implemented according to the $\tilde{t} \to \tilde{t}g$ splitting function given above (see also ref. [53]), together with some additional features such as angular ordering of the gluon shower due to soft gluon interference as described in ref. [54]. The formation and decay of the $\tilde{t}$ hadron is then implemented in the spectator quark approach [55]. After the decay, a color string is pulled between the decay c quark and the spectator quark, giving rise to the standard string fragmentation.

The user can choose the values of the center of mass energy, the $\tilde{t}$ mass, the mixing angle $\theta_{\tilde{t}}$, and the $\tilde{\chi}_1^0$ mass. It is also possible to decide whether or not to include QCD corrections and/or initial state radiation. The decay $\tilde{t} \to b\tilde{\chi}_1^+$ with $\tilde{\chi}_1^+ \to W^* \tilde{\chi}_1^0 \to f\bar{f}'\tilde{\chi}_1^0$ is also implemented; in this case, the $\tilde{\chi}_1^+$ mass is an additional free input parameter.

The $\tilde{b}$ event generator has been implemented along similar lines; the only decay mode in this case is $\tilde{b}_1 \to b\tilde{\chi}_1^0$.

3.6.2 The L3 event generator.

The L3 event generator [51] includes both $\tilde{\chi}^0$ and $\tilde{\chi}^{\pm}$ decay modes. The L3 event generator is based on the calculation of 4-momenta distributions of the final state particles $\tilde{\chi}_1^0 c \tilde{\chi}_1^0 \bar{c}$ or $\tilde{\chi}_1^- b \tilde{\chi}_1^+ \bar{b}$. The large effects of QCD corrections are included in the cross section calculations using the results of ref. [56] (see also [53]). The $\tilde{t}$ production and decay have been defined as new processes in PYTHIA [16]. The event generation process includes modeling of hadronic final states.

In the first step of the event generation, initial state photons are emitted using the program package REMT [16], and the production cross section at the reduced center-of-mass energy is calculated. The effective center-of-mass energy is calculated for the generation of the 4-momenta of the final state particles. These 4-momenta are then boosted according to the momentum of the initial state photon. No perturbative gluon radiation is included before the $\tilde{t}$ decay. This is justified by the fact that less than about 1% of the $\tilde{t}$ energy is expected to be radiated in the form of hard gluons. After the $\tilde{t}$ decay, a color string with the invariant mass of the quark-antiquark-system ($c\bar{c}$ or $b\bar{b}$) is defined. Gluon emission and hadronization is then performed using the Lund model of string fragmentation as implemented in PYTHIA [16]. The Peterson fragmentation parameters [61] for the c and b-quarks are chosen to be $\epsilon_c = 0.03$ and $\epsilon_b = 0.0035$, as determined from L3 event shape distributions. Finally, short-lived particles decay into their observable final state, where the standard L3 particle decay tables are applied.

3.6.3 The OPAL event generator.

The OPAL event generator has been used by OPAL [58] in the LEP1 analyses of $\tilde{t}$ search. It only includes the $\tilde{t} \to c\tilde{\chi}_1^0$ decay. The production matrix elements are taken from ref. [29, 57], including the effect of QCD corrections. In the first step of the event generation, inital state photons are emitted taking into account the $\tilde{t}\bar{\tilde{t}}$ cross section at the reduced center of mass energy. JETSET [16] is then used to perform the perturbative gluon emission. This is done using the default emission probabilities, evaluated assuming the radiating particle to have spin-1/2. After the perturbative evolution, Peterson fragmentation is introduced, with the parameter $\epsilon_{\tilde{t}}$ set to

$$\epsilon_{\tilde{t}} = \epsilon_b \frac{m_b^2}{m_{\tilde{t}}^2}, \quad \epsilon_b = 0.0057, \; m_b = 5 \text{ GeV}. \tag{3.5}$$

As mentioned above, in the case of the $\tilde{t} \to c\tilde{\chi}_1^0$ decay the $\tilde{t}$ hadronizes to form a $\tilde{t}$-hadron before it decays. $\tilde{t}$-hadrons are therefore formed, as bound states of a $\tilde{t}$ and a light anti-quark ($\bar{u}$, $\bar{d}$), $\bar{s}$, or a diquark (uu etc.). As a result of the combined perturbative and non-perturbative evolution, about 1% [0.5%] of the $\tilde{t}$ initial energy goes into ordinary hadrons for a 70 GeV (80 GeV) $\tilde{t}$ at $\sqrt{s} = 190$ GeV. This is consistent with the estimates given earlier.

After the $\tilde{t}$ decay, a colour string is stretched between the charm quark and the spectator. This colour singlet system is again hadronized by JETSET. Additional gluon bremsstrahlung

is allowed in this process. The Peterson fragmentation function is used at the end of the charm quark evolution.

A code based on the same physical principles was also developed by ALEPH, and has been used in their LEP1 $\tilde{t}$ analysis [59].

3.6.4 Comparison of generators for $\tilde{t}\bar{\tilde{t}}$.

We now compare some details of the OPAL, DELPHI, and L3 $\tilde{t}\bar{\tilde{t}}$ generators for the $\tilde{\chi}_1^0 c \tilde{\chi}_1^0 \bar{c}$ channel. Some differences in the features of the final states are observed, and their origin can be found in the different treatment of the hadronization process. In the L3 generator, $\tilde{t}$ production and decay is performed in analogy to the top quark, whose lifetime is much shorter than the hadronization time scale. Connecting the final state c and $\bar{c}$ with a string implicitly assumes that the $c\bar{c}$ system will radiate coherently. This is not the case for radiation whose wave-length is smaller than the $\tilde{t}$ lifetime. OPAL introduces the intermediate step of $\tilde{t}$-hadron formation. The radiating system after $\tilde{t}$ decay is then given not by the $c\bar{c}$ pair, but by the two systems $c\bar{q}$ and $\bar{c}q'$, q and q' being the spectator quarks. Qualitalively this will lead to lower particle multiplicity and more collimated jets than in the L3 approach. DELPHI introduces the emission of a large number of low energy gluons to simulate the fragmentation of the stop bound state. In all codes, we have checked that the effect of varying the ϵ parameter in the Peterson fragmentation effects is very small.

To illustrate the effect of the differences just mentioned, Table 18 shows the total final state charged and neutral multiplicities, as obtained from the different programs. Table 19 shows multiplicities, energies and masses for particles with a minimum energy of 500 MeV, *i.e.* above the typical detector thresholds. The visible energy is essentially determined by the decay kinematics of the $\tilde{t}$ hadron. The 3-5 GeV difference between the OPAL and L3 generators is due to the energy of hadrons produced during the QCD evolution of the $\tilde{t}$ before it hadronizes. This difference increases for lighter $\tilde{t}$ because of the softer fragmentation function. The particle multiplicity found by L3 is larger than OPAL's by up to 4 charged particles per event, depending on the $\tilde{t}$ and $\tilde{\chi}^0$ masses. This is consistent with what anticipated above. The two-jet structure is expected to be clearer for events generated by OPAL than L3 and DELPHI, because the jet evolution is localized in the $\tilde{t}$-hadron decay. In the DELPHI generator, the cut-off for the gluon emission is a critical parameter and may explain the larger visible energy. The matching of the evolution scale Q^2 where to terminate the gluon emission with the Q_0^2 parameter in the Lund QCD parton shower optimized for the Lund string fragmentation model must be investigated for the DELPHI model.

The DELPHI and L3 generators also include the $b\tilde{\chi}_1^+ \bar{b}\tilde{\chi}_1^-$ channel. A comparison between them appears in table 20. The agreement is good, because the $\tilde{\chi}_1^+$ decay is described in a similar way in the two generators, and in both cases the hadronization takes place in the $b\bar{b}$ system.

The $\tilde{t}$-search studies are documented in [5]. Since the global event signature is the large missing momentum due to the presence of two neutralinos in the final state, the variables in the

(70,50)	neutral	charged	Evis	Mvis
OPAL	10	8.1	50	41
DELPHI	22	19	56	46
L3	15	12	48	37

Table 18: Comparison of LEP2 generators in the $\tilde{\chi}_1^0 c \tilde{\chi}_1^0 \bar{c}$ channel: neutral and charged multiplicity, visible energy (in GeV) and visible mass (in GeV) without a cut on the particle energy. Stop and neutralino masses (in GeV) are given in brackets.

event analysis can be chosen to be largely independent of the generator differences. Differences related to the hadronization properties, which possibly affect the jet structure, can be overcome by choosing different resolution parameters in the jet definitions. As a net result, in spite of the differences currently observed among these three generators the studies of the $\tilde{t}$ discovery potential carried out by the three experiments are consistent with each other [5].

4 Leptoquarks

4.1 LQ2

Program name:	LQ2 – Leptoquark Event Generator 1.00/04
Date of last revision:	29 September 1995
Author:	D. M. Gingrich – `gingrich@phys.ualberta.ca`
Other programs called:	JETSET 7.405 (plus PYTHIA 5.710) and CERNLIB (DIVON4, RANECU)
Comments:	source code managed with CMZ
Availability:	The complete code documentation is available from the author

This section describes a Monte Carlo program which generates pair production of scalar or vector leptoquarks in electron-positron annihilation. The leptoquarks are produced according to an effective Lagrangian with the following properties [62]: 1) baryon and lepton number conservation, 2) non-derivative and family diagonal couplings to lepton-quark pairs and 3) $SU(3)_C \times SU(2)_L \times U(1)_Y$ invariance.

The contributions to leptoquark pair production from the s-channel exchange of an electroweak boson, t-channel exchange of a quark and the interference between them are included in the differential cross-section. The angular distribution of the scalar or vector leptoquarks assumes unpolarized beams. Initial state radiation, currently not present, will soon be included. The centre of mass energy is not restricted to the Z-resonance. The leptoquarks are allowed

(70,50)	neutral	charged	Evis	Mvis
OPAL	6.6	7.0	48	39
DELPHI	10	16	53	43
L3	9.0	11	45	35
(70,60)	neutral	charged	Evis	Mvis
OPAL	5.0	5.8	28	23
DELPHI	8.3	14	35	28
L3	6.5	7.7	24	19
(70,65)	neutral	charged	Evis	Mvis
OPAL	3.7	4.8	17	14
DELPHI	6.1	11	24	19
L3	4.1	5.3	12	9.6

Table 19: Comparison of LEP2 generators in the $\tilde{\chi}_1^0 c \tilde{\chi}_1^0 \bar{c}$ channel: neutral and charged multiplicity, visible energy (in GeV) and visible mass (in GeV) with a minimum cut on the particle energy of 500 MeV. Stop and neutralino masses (in GeV) are given in brackets.

(70,60,30)	neutral	charged	Evis	Mvis
DELPHI	17	21	81	76
L3	15	20	79	74

Table 20: Comparison of LEP2 generators in the $b\tilde{\chi}_1^+ \bar{b}\tilde{\chi}_1^-$ channel: neutral and charged multiplicity, visible energy (in GeV) and visible mass (in GeV) with a minimum cut on the particle energy of 500 MeV. Stop and neutralino masses (in GeV) are given in brackets.

to decay to lepton-quark or neutrino-quark final states. Decays to all three generations are possible but the massless quark approximation will not be valid for decays to the top quark.

The LUND routines of JETSET [16] are used for the final state parton shower, fragmentation and decay processes. The generator fills the JETSET common block /LUJETS/ and the standard Monte Carlo generator common block /HEPEVT/. The mechanics of the program closely follows that of an analogous generator for simulating leptoquark production and decay in electron-proton collisions [63].

Physics Processes. The lowest order Feynman diagrams for leptoquark production in electron-positron annihilation ($e^+e^- \to L_Q\overline{L_Q}$) are straightforward to evaluate using the general couplings from the effective Lagrangian [62]. In general, the pair production amplitudes for the s-channel and t-channel processes can interfere and the differential cross-section for the production of scalar leptoquarks is given by three terms:

$$\frac{d\sigma_{\rm scalar}}{d(\cos\theta)} = \frac{3\pi\alpha^2}{8s}\beta^3\sin^2\theta \sum_{a=\rm L,R}[|A_\gamma + A_{\rm Z}|^2_a + 2\lambda^2_a Re[(A_\gamma + A_{\rm Z})_a(A^*_{\rm q})_a] + \lambda^4_a|A_{\rm q}|^2_a], \qquad (4.1)$$

where A_γ and $A_{\rm Z}$ denote the photon and Z-boson s-channel exchange terms, and $A_{\rm q}$ is the t-channel exchange term. The sum is over electron polarizations and $\lambda_{\rm L,R}$ are the generalized couplings. θ is the polar angle and $\beta = \sqrt{1-4m^2_{\rm LQ}/s}$ is a kinematic threshold factor.

Similarly the differential cross-section for the production of vector leptoquarks is

$$\frac{d\sigma_{\rm vector}}{d(\cos\theta)} = \frac{3\pi\alpha^2}{8M^2_{LQ}}\beta^3\left(\frac{7-3\beta^2}{4}\right)\sum_{a=\rm L,R}[|A_\gamma + A_{\rm Z}|^2_a + 2\lambda^2_a Re[(A_\gamma + A_{\rm Z})_a(A^*_{\rm q})_a] + \lambda^4_a|A_{\rm q}|^2_a], \quad (4.2)$$

From the effective lagrangian one can obtain the various partial leptoquark decay widths, $\Gamma_{\rm LQ}$. For the scalar (S) and vector (V) leptoquarks we have

$$\Gamma^{\rm S}_{\rm LQ} = \frac{\lambda^2_{\rm L,R}m_{\rm LQ}}{16\pi} \quad \text{and} \quad \Gamma^{\rm V}_{\rm LQ} = \frac{\lambda^2_{\rm L,R}m_{\rm LQ}}{24\pi}, \qquad (4.3)$$

where $\lambda_{\rm L,R}$ denote the leptoquark couplings to a particular final state and $m_{\rm LQ}$ is the leptoquark mass. The total widths are obtained by summing over all possible final states.

Table 21 gives the quantum numbers, couplings and decay channels for all leptoquarks. We have adapted the notation of ref. [64][3].

Generator. The user must supply his own main program to initialize the package and generate events. The initialization routine LQINIT must be called once to perform some initialization and calculate the total cross-section. Some simple checks are make to see that the required leptoquark and decay process are consistent with the requested quantum numbers and couplings.

[3] $S_0, \tilde{S}_0, S_1, V_{1/2}, \tilde{V}_{1/2}, V_0, \tilde{V}_0, V_1, S_{1/2}, \tilde{S}_{1/2}$ in ref. [64] correspond to $S_1, \tilde{S}_1, S_3, V_2, \tilde{V}_2, U_1, \tilde{U}_1, U_3, R_2, \tilde{R}_2$ in ref. [62] respectively.

A call is automatically made to the routine TOTSCALAR or TOTVECTOR to calculate the total cross-section. The differential cross-section function XSCALAR or XVECTOR is numerically integrated as a test that the generator is initialized properly. The resonance width and branching ratio are also calculated. A program banner, the value of some parameters and the process to be generated are printed out.

Events are generated by calling the routine LQGEN once per event in the user main program. The routine to create the event record, LQFILL, is then automatically called by LQGEN. Routines from JETSET are used for final state fragmentation and decay processes.

All other subroutines and functions are called internally. But, if so desired, the total cross-section functions or differential cross-section functions (function of polar angle) may be called by the user after initialization.

Numerical integration. The differential cross-sections are integrated and sampled using the CERNLIB package DIVON4 [65]. The package consists of a collection of routines to aid in the numerical integration of functions of several variables and to sample points in a multi-dimensional coordinate space from a specified probability density function. The algorithm adaptively partitions a multi-dimensional coordinate space into a set of axis-oriented hyper-rectangular regions, based on a user provided function. These regions are then used for a stratified sampling estimate of the integral of the function, or to sample random vectors from the coordinate space with probability density that of the function. The integration and importance sampling are extremely fast in LQ2 since the cross-section is a function of a single variable.

Installation and availability. The LQ2 package is managed as a CMZ library. The program needs to be linked with JETSET version 7.4 and PYTHIA version 5.7. The CERN libraries MATHLIB and KERNLIB must also be loaded to include the random number generator RANECU timing routine TIMED and the integration package DIVON4.

The LQ2 CMZ library can be obtained via anonymous ftp at `jever.phys.ualberta.ca` in file `pub/lq2.cmz`.

${}^{Q}\mathrm{LQ}_{T}$	T_3	*Decay*	*Coupling*
${}^{-1/3}\mathrm{S}_0$	0	$\mathrm{e}_\mathrm{L}^- \mathrm{u}_\mathrm{L}$	λ_L
${}^{-1/3}\mathrm{S}_0$	0	$\mathrm{e}_\mathrm{R}^- \mathrm{u}_\mathrm{R}$	λ_R
${}^{-1/3}\mathrm{S}_0$	0	$\nu_\mathrm{e} \mathrm{d}_\mathrm{L}$	$-\lambda_\mathrm{L}$
${}^{-4/3}\tilde{\mathrm{S}}_0$	0	$\mathrm{e}_\mathrm{R}^- \mathrm{d}_\mathrm{R}$	λ_R
${}^{+2/3}\mathrm{S}_1$	$+1$	$\nu_\mathrm{e} \mathrm{u}_\mathrm{L}$	$\sqrt{2}\lambda_\mathrm{L}$
${}^{-1/3}\mathrm{S}_1$	0	$\nu_\mathrm{e} \mathrm{d}_\mathrm{L}$	$-\lambda_\mathrm{L}$
${}^{-1/3}\mathrm{S}_1$	0	$\mathrm{e}_\mathrm{L}^- \mathrm{u}_\mathrm{L}$	$-\lambda_\mathrm{L}$
${}^{-4/3}\mathrm{S}_1$	-1	$\mathrm{e}_\mathrm{L}^- \mathrm{d}_\mathrm{L}$	$-\sqrt{2}\lambda_\mathrm{L}$
${}^{-1/3}\mathrm{V}_{1/2}$	$+1/2$	$\nu_\mathrm{e} \mathrm{d}_\mathrm{R}$	λ_L
${}^{-1/3}\mathrm{V}_{1/2}$	$+1/2$	$\mathrm{e}_\mathrm{R}^- \mathrm{u}_\mathrm{L}$	λ_R
${}^{-4/3}\mathrm{V}_{1/2}$	$-1/2$	$\mathrm{e}_\mathrm{L}^- \mathrm{d}_\mathrm{R}$	λ_L
${}^{-4/3}\mathrm{V}_{1/2}$	$-1/2$	$\mathrm{e}_\mathrm{R}^- \mathrm{d}_\mathrm{L}$	λ_R
${}^{+2/3}\tilde{\mathrm{V}}_{1/2}$	$+1/2$	$\nu_\mathrm{e} \mathrm{u}_\mathrm{R}$	λ_L
${}^{-1/3}\tilde{\mathrm{V}}_{1/2}$	$-1/2$	$\mathrm{e}_\mathrm{L}^- \mathrm{u}_\mathrm{R}$	λ_L
${}^{-2/3}\mathrm{V}_0$	0	$\mathrm{e}_\mathrm{L}^- \overline{\mathrm{d}}_\mathrm{R}$	λ_L
${}^{-2/3}\mathrm{V}_0$	0	$\mathrm{e}_\mathrm{R}^- \overline{\mathrm{d}}_\mathrm{L}$	λ_R
${}^{-2/3}\mathrm{V}_0$	0	$\nu_\mathrm{e} \overline{\mathrm{u}}_\mathrm{R}$	λ_L
${}^{-5/3}\tilde{\mathrm{V}}_0$	0	$\mathrm{e}_\mathrm{R}^- \overline{\mathrm{u}}_\mathrm{L}$	λ_R
${}^{+1/3}\mathrm{V}_1$	$+1$	$\nu_\mathrm{e} \overline{\mathrm{d}}_\mathrm{R}$	$\sqrt{2}\lambda_\mathrm{L}$
${}^{-2/3}\mathrm{V}_1$	0	$\mathrm{e}_\mathrm{L}^- \overline{\mathrm{d}}_\mathrm{R}$	$-\lambda_\mathrm{L}$
${}^{-2/3}\mathrm{V}_1$	0	$\nu_\mathrm{e} \overline{\mathrm{u}}_\mathrm{R}$	λ_L
${}^{-5/3}\mathrm{V}_1$	-1	$\mathrm{e}_\mathrm{L}^- \overline{\mathrm{u}}_\mathrm{R}$	$\sqrt{2}\lambda_\mathrm{L}$
${}^{-2/3}\mathrm{S}_{1/2}$	$+1/2$	$\nu_\mathrm{e} \overline{\mathrm{u}}_\mathrm{L}$	λ_L
${}^{-2/3}\mathrm{S}_{1/2}$	$+1/2$	$\mathrm{e}_\mathrm{R}^- \overline{\mathrm{d}}_\mathrm{R}$	$-\lambda_\mathrm{R}$
${}^{-5/3}\mathrm{S}_{1/2}$	$-1/2$	$\mathrm{e}_\mathrm{L}^- \overline{\mathrm{u}}_\mathrm{L}$	λ_L
${}^{-5/3}\mathrm{S}_{1/2}$	$-1/2$	$\mathrm{e}_\mathrm{R}^- \overline{\mathrm{u}}_\mathrm{R}$	λ_R
${}^{+1/3}\tilde{\mathrm{S}}_{1/2}$	$+1/2$	$\nu_\mathrm{e} \overline{\mathrm{d}}_\mathrm{L}$	λ_L
${}^{-2/3}\tilde{\mathrm{S}}_{1/2}$	$-1/2$	$\mathrm{e}_\mathrm{L}^- \overline{\mathrm{d}}_\mathrm{L}$	λ_L

Table 21: Quantum numbers (Q is the electric charge, T is the weak isospin and T_3 is the third component of isospin), coupling constants and decay channels for leptoquarks.

References

[1] See the "Higgs Physics" Chapter in vol. I of this Report.

[2] See the "Event generators for WW physics" Chapter in this volume.

[3] M. Consoli, W. Hollik and F. Jegerlehner in: Z Physics at LEP1, G. Altarelli, R. Kleiss and C. Verzegnassi eds., CERN Yellow Report No.89-08 (1989) Vol. 1, p.7.

[4] E. Gross, B.A. Kniehl and G. Wolf, *Z. Phys.* **C63** (1994) 417.

[5] See the "Search for New Physics" Chapter in vol. I of this Report.

[6] E. Boos, M. Dubinin, V. Edneral, V. Ilyin, A. Kryukov, A. Pukhov, S. Shichanin, in: "New Computing Techniques in Physics Research II", ed.by D. Perret-Gallix, World Scientific, Singapore, 1992, p. 665
in: Proc. of the XXVI Recontre de Moriond, ed. by Tranh Than Van, Editions Frontieres, 1991, p. 501;
E.Boos, M.Dubinin, V.Ilyin, A.Pukhov, V.Savrin, preprint INP MSU 94-36/358, 1994 (hep-ph/9503280)

[7] S. Kawabata, *Comput. Phys. Commun.* **41** (1986) 127; *ibid.* **88** (1995) 309

[8] E.Boos, M.Sachwitz, H.J.Schreiber, S.Shichanin, *Z. Phys.* **C61** (1994) 675;
M.Dubinin, V.Edneral, Y.Kurihara, Y.Shimizu, *Phys. Lett.* **B329** (1994) 379;
E.Boos, M.Sachwitz, H.J.Schreiber, S.Shichanin, *Int. Jour. Mod. Phys.* **A10** (1995) 2067;
E.Boos, M.Sachwitz, H.J.Schreiber, S.Shichanin, *Z. Phys.* **C64** (1994) 361;
E.Boos, M.Sachwitz, H.J.Schreiber, S.Shichanin, DESY preprint 95-002, 1995.

[9] D. Bardin, A. Leike and T. Riemann, *Phys. Lett.* **B344** (1995) 383.

[10] D. Bardin, A. Leike and T. Riemann, *Phys. Lett.* **B353** (1995) 513.

[11] Review of particle properties, L. Montanet et al., *Phys. Rev.* **D50** (1994) 1173.

[12] G. Montagna, O. Nicrosini and F. Piccinini, *Phys. Lett.* **B348** (1995) 496.

[13] HIGGSPV - in preparation.

[14] M. Carena, M. Quiros, and C.E.M. Wagner, CERN preprint CERN-TH/95-157.

[15] H. Haber, R. Hempfling and A. Hoang, private commmunication.

[16] T. Sjöstrand, *Comput. Phys. Commun.* **82** (1994) 74.

[17] A. Ballestrero, E. Maina, *Phys. Lett.* **B350** (1995) 225.

[18] A. Ballestrero, in preparation.

[19] F.A. Berends, P.H. Daverveldt and R. Kleiss, *Nucl. Phys.* **B253** (1985) 441;
R. Kleiss and W.J. Stirling, *Nucl. Phys.* **B262** (1985) 235.

[20] G.P. Lepage, *Jour. Comp. Phys.* **27** (1978) 192.

[21] D. Bardin et al. in Physics at LEP200 and Beyond, *Nucl. Phys.* **37B** (Proc. Suppl.) (1994), T. Riemann and J. Blümlein eds.

[22] G. Montagna, O. Nicrosini, G. Passarino and F. Piccinini, *Phys. Lett.* **B348** (1995) 178.

[23] G. Montagna, O. Nicrosini and F. Piccinini, *Comput. Phys. Commun.* **90** (1995) 141.

[24] F. A. Berends, R. Kleiss and R. Pittau, *Nucl. Phys.* **B426** (1994) 344.

[25] D. Bardin, W. Beenakker and A. Denner, *Phys. Lett.* **B137** (1993) 213.

[26] G. Passarino, *Nucl. Phys.* **B237** (1984) 249.

[27] J. Hilgart, R. Kleiss and F. Le Diberder, *Comput. Phys. Commun.* **75** (1993) 191.

[28] For references see the review papers: H.-P. Nilles, *Phys. Rep.* **110** (1984) 1;
H.E. Haber, G.L. Kane, *Phys. Rep.* **117** (1985) 75;
R. Barbieri, *Riv. Nuo. Cim.* **11** (1988) 1.

[29] M. Drees and K. Hikasa, *Phys. Lett.* **B252** (1990) 127.

[30] J. Ellis, G. Ridolfi and F. Zwirner, *Phys. Lett.* **B257** (1991) 83; *Phys. Lett.* **B262** (1991) 477.

[31] A. Bartl, H. Fraas, W. Majerotto, *Z. Phys.* **C30** (1986) 411; *Z. Phys.* **C34** (1987) 411; *Z. Phys.* **C41** (1988) 475, *Nucl. Phys.* **B278** (1986) 1; *Z. Phys.* **C55** (1992) 257.

[32] S. Ambrosanio and B. Mele, *Phys. Rev.* **D52** (1995) 3900, and ROME1-1095/95 hep-ph/9508237.

[33] H. Dreiner and S. Lola, DESY 92-123B, p 707.

[34] F. Paige and S. Protopopescu, in *Supercollider Physics*, p. 41, ed. D. Soper (World Scientific, 1986);
H. Baer, F. Paige, S. Protopopescu and X. Tata, in *Proceedings of the Workshop on Physics at Current Accelerators and Supercolliders*, ed. J. Hewett, A. White and D. Zeppenfeld, (Argonne National Laboratory, 1993).

[35] G. Fox and S. Wolfram, *Nucl. Phys.* **B168** (1980) 285.

[36] R. Field and R. Feynman, *Nucl. Phys.* **B136** (1978) 1.

[37] Y. Okada, M. Yamaguchi and T. Yanagida, *Phys. Lett.* **262B** (1991) 54;
H. Haber and R. Hempfling, *Phys. Rev. Lett.* **66** (1991) 1815; J. Ellis, G. Ridolfi and F. Zwirner, *Phys. Lett.* **257B** (1991) 83;
for detailed formulae incorporated into ISAJET, see M. Bisset, University of Hawaii Ph. D. Thesis UH-511-813-94 (1994).

[38] H. Baer, C. H. Chen, R. Munroe, F. Paige and X. Tata, *Phys. Rev.* **D51** (1995) 1046.

[39] H. Baer, A. Bartl, D. Karatas, W. Majerotto and X. Tata, *Int. Jour. Mod. Phys.* **A4** (1989) 4111.

[40] H. Baer, M. Brhlik, R. Munroe and X. Tata, *Phys. Rev.* **D52** (1995) 5031.

[41] Y. Kurihara, J. Fujimoto, T. Munehisa, Y. Shimizu, "QEDPS" in this Yellow Report: KEK CP-035, KEK Preprint 95-126, 1995

[42] Minami-Tateya collabolation, "GRACE manual ver 1.0", KEK Report **92-19**, 1993;
Minami-Tateya collabolation, Brief Manual of GRACE system ver $2.0/\beta$, 1995.

[43] K. Hikasa, *JLC Supersymmetry Manual*, unpublished.

[44] M.Chen,C.Dionisi,M.Martinez and X.Tata, *Phys. Rep.* **159** (1988) 201;
C.Dionisi et al., Proc. of the ECFA workshop on LEP 200, Aachen, 1986, Vol.II, p. 380, CERN 87-08, ECFA;
A.Bartl, H.Fraas, W. Majerotto and B. Mösslacher, *Z. Phys.* **C55** (1992) 257.

[45] C. Dionisi, K. Fujii, S. Giagu and T. Tsukamoto, in preparation.

[46] H. Murayama, I. Watanabe and K. Hagiwara, KEK Preprint 91-11 (1992)

[47] J.Fujimoto et al., *Progr. of Theor. Phys.*, Supplement No. 100 (1990), Equation (11.200) on p297.

[48] S. Katsanevas and S. Melachroinos, "SUSYGEN" in this Yellow Report

[49] Ya.I. Azimov, Yu.L. Dokshitzer and V.A. Khoze, *Yad. Fiz.* **36** (1982) 1510.

[50] M. Besançon, DELPHI Note, in preparation.

[51] A. Sopczak, L3 Note 1860, (1995). The generator is implemented in the L3 software under the name `EGLOv201`.

[52] S. Asai, S. Komamiya and S. Orito, preprint UT-ICEPP 95-10 (1995).

[53] W.Beenakker, R. Hopker and P.M. Zerwas, *Phys. Lett.* **B349** (1995) 468.

[54] G.Marchesini and R.B.Webber, *Nucl. Phys.* **B310** (1988) 461.

[55] A. Ali, *Z. Phys.* **C1** (1979) 25;
M.K. Gaillard, B.W. Lee and J.L. Rosner, *Rev. Mod. Phys.* **47** (1975) 227;
V. Barger, T. Gottschalk and R.J.N Phillips, *Phys. Lett.* **B82** (1979) 445;
M. Suzuki, *Nucl. Phys.* **B258** (1985) 553.

[56] A. Bartl, W. Majerotto, W. Porod, *Z. Phys.* **C64** (1994) 499, and private communication.

[57] K. Hikasa and M. Kobayashi, *Phys. Rev.* **D36** (1987) 724.

[58] OPAL Collaboration, R. Akers *et al.*, *Phys. Lett.* **B337** (1994) 207.

[59] ALEPH Collaboration, Proc. of the International Europhysics Conference on High Energy Physics, Brussels, Belgium, 27 July - 2 August (1995).

[60] B. Andersson *et al.*, *Phys. Rep.* **97** (1983) 31.

[61] C. Peterson, D. Schlatter, I. Schmitt and P.M. Zerwas, *Phys. Rev.* **D27** (1983) 105.

[62] J. Blümlein & R. Rückl, *Phys. Lett.* **B304** (1993) 337.

[63] D.M. Gingrich, Oxford University preprint OUNP-92-19;
D. Gingrich & N. Harnew, Proceedings of the Workshop, 29-30 Oct. 1991, Hamburg, ed. W. Buchmüller & G. Ingelman, Vol. 3, pp. 1542-1550.

[64] T. Köhler, Diplomarbeit at the RWTH Aachen (1989);
B. Schrempp, Proceedings of the Workshop, 29-30 Oct. 1991, Hamburg, ed. W. Buchmüller & G. Ingelman, Vol. 2, pp. 1034-1042.

[65] J.H. Friedman & M.H. Wright, "DIVONNE4 – A Program for Multiple Integration and Adaptive Importance Sampling", CERN D151 DIVON4, 1981.06.01.

[66] "A Source Code Management System CMZ", version 1.37, 1991.07.13.